NASA TECHNICAL NOTE

NASA TN D-2835

NASA TN D-2835

GEOMETRIC SHAPE FACTORS FOR PLANETARY-THERMAL AND PLANETARY-REFLECTED RADIATION INCIDENT UPON SPINNING AND NONSPINNING SPACECRAFT

by Lenwood G. Clark and E. Clay Anderson

Langley Research Center
Langley Station, Hampton, Va.

NATIONAL AERONAUTICS AND SPACE ADMINISTRATION • WASHINGTON, D. C. • MAY 1965

NASA TN D-2835

GEOMETRIC SHAPE FACTORS FOR PLANETARY-THERMAL AND PLANETARY-REFLECTED RADIATION INCIDENT UPON SPINNING AND NONSPINNING SPACECRAFT

By Lenwood G. Clark and E. Clay Anderson

Langley Research Center
Langley Station, Hampton, Va.

NATIONAL AERONAUTICS AND SPACE ADMINISTRATION

For sale by the Clearinghouse for Federal Scientific and Technical Information
Springfield, Virginia 22151 – Price $3.00

GEOMETRIC SHAPE FACTORS FOR PLANETARY-THERMAL AND PLANETARY-REFLECTED RADIATION INCIDENT UPON SPINNING AND NONSPINNING SPACECRAFT

By Lenwood G. Clark and E. Clay Anderson
Langley Research Center

SUMMARY

Truncated series expressions are obtained for the planetary-thermal and planetary-reflected solar radiation incident upon arbitrarily oriented spinning and nonspinning spacecraft. For the spinning case, spacecraft having the angular momentum vector either normal to or coincident with the axis of symmetry are considered. Results are presented in graphical form for planar surfaces and bodies of revolution as a function of spacecraft attitude and altitude. Results for the spinning case are obtained by averaging instantaneous values over a spin period and are sufficiently accurate for most spinning spacecraft. Expressions for obtaining the spacecraft's attitude in terms of orbit parameters for the solar-oriented case are included.

INTRODUCTION

In order to maintain the temperatures of many components of spacecraft within specified limits, the thermal design of the spacecraft must be based on an accurate description of the radiant heat flux incident to the vehicle. The sources of radiant heat flux incident upon an orbiting spacecraft are: direct solar radiation, planetary-reflected solar radiation, and planetary-thermal radiation. The magnitudes of these heat fluxes are influenced by the appropriate geometric shape factors which vary with altitude and attitude.

Since an orbiting spacecraft is located at a great distance from the sun, the geometric shape factor for direct solar radiation is the easiest to calculate and is defined by projection of the vehicle area element in question in the direction of the sun. However, the geometric shape factors for planetary-thermal and planetary-reflected solar radiation are dependent upon both altitude and attitude and thus are more difficult to determine.

Geometric shape factors for planetary-thermal and planetary-reflected solar radiation are given as integral expressions in references 1 to 4 for several geometric configurations. The solution of these equations, however, requires the use of digital computers. References 1 to 3 consider various geometric configurations for both the spin and nonspin modes of operation but

present a limited amount of data. Reference 4 presents data for the nonspin case only.

This report presents truncated series representations for the geometric shape factors for planetary-thermal and planetary-reflected solar radiation incident upon arbitrarily oriented planar surfaces and bodies of revolution. Each configuration is considered for both the spin and nonspin modes of operation and results are presented in graphical form as a function of the spacecraft's altitude and attitude. The results of this study are of value in the thermal design of any orbiting spacecraft, spinning or nonspinning, since they can be used to predict the approximate radiant heat flux incident to the vehicle and thus assist in the design of temperature control systems.

Expressions for obtaining the spacecraft's attitude in terms of orbit parameters for the solar-oriented case are derived in an appendix.

SYMBOLS

A	surface area
a	planetary albedo, dimensionless
C_s	solar constant
F	geometric shape factor, dimensionless
H	distance between spacecraft and center of planet, $R + h$
$\overline{H}$	spacecraft angular momentum vector
h	orbit altitude
I	orbit inclination measured from planet equatorial plane
i	ecliptic inclination measured from planet equatorial plane
J	radiant heat intensity
M	rotational matrix
N	integer
$\overline{N}$	unit normal vector to spacecraft surface element
q	radiant heat flux incident upon spacecraft surface area
R	mean radius of planet
$\overline{R}$	vector from spacecraft to center of planet

α angle between line from spacecraft to center of planet and line from spacecraft to element on planet surface

β right ascension of ascending orbit node measured in planet equatorial plane (zero at vernal equinox)

γ spacecraft position angle measured in orbit plane (zero at ascending orbit node), $\gamma_p + \eta$

γ_p argument of orbit perigee measured in orbit plane (zero at ascending orbit node)

δ semiapex angle

ϵ orbit eccentricity, dimensionless

η spacecraft position angle measured in orbit plane (zero at orbit perigee)

η_s angle between line from center of planet to sun and line from center of planet to spacecraft

θ angle between spacecraft axis of symmetry and line from spacecraft to center of planet

Λ angle between vector normal to spacecraft surface element and line from spacecraft to element on planet surface

λ angle between vector normal to spacecraft surface element and line from spacecraft to center of planet

ν angle of rotation about either spacecraft orientation vector or spacecraft angular momentum vector

ξ angle of rotation of spacecraft surface element about spacecraft axis of symmetry measured from either spacecraft orientation vector or spacecraft angular momentum vector

ρ distance between spacecraft and element on planet surface

Φ angle between spacecraft angular momentum vector and line from spacecraft to center of planet

φ azimuth angle in spherical coordinates

Ω position angle of sun measured in the ecliptic plane (zero at vernal equinox)

Subscripts:

ent shadow entrance

exit	shadow exit
gen	general
L	limit
p	perigee
R	planetary-reflected solar
s	solar
T	planetary thermal

ANALYSIS

Planetary-Thermal Radiation

The planetary-thermal radiant heat energy incident upon a vehicle surface area A is given by

$$q_T = J_T AF \tag{1}$$

where J_T is the thermal radiation intensity of a spherical planet assumed to radiate according to Lambert's cosine law. With this assumption

$$J_T = \frac{C_s(1 - a)}{4} \tag{2}$$

Planetary-Reflected Solar Radiation

If it is assumed that the planet is a diffuse reflector of solar radiation and that the geometric shape factor for planetary-reflected solar radiation is, from reference 5, approximately given by

$$F_R = F \cos \eta_s \tag{3}$$

then the planetary-reflected solar radiant heat energy incident upon a vehicle surface area is given by

$$q_R = J_R AF \cos \eta_s \tag{4}$$

where

$$\left.\begin{aligned} J_R &= C_s a \qquad \left(-\frac{\pi}{2} < \eta_s < \frac{\pi}{2}\right) \\ J_R &= 0 \qquad \left(\frac{\pi}{2} \leqq \eta_s \leqq \frac{3\pi}{2}\right) \end{aligned}\right\} \tag{5}$$

The evaluation of equations (1) and (4) requires knowledge of the geometric shape factor for planetary-thermal radiation F. The following section of this report is concerned with the derivation of this parameter for several spacecraft configurations.

Geometric Shape Factor

Planar configuration.- For two black surfaces separated by a nonabsorbing medium, the geometric shape factor F_{12} from surface A_1 to surface A_2 is defined as the fraction of the total radiant flux leaving A_1 that is incident upon A_2 and is given for $A_1 \ll A_2$ from reference 6 by

$$F_{12} = \frac{1}{A_1} \int_{A_2} \frac{A_p(\Lambda)\cos\alpha}{\pi\rho^2}\, dA_2 \tag{6}$$

where $A_p(\Lambda)$ is the projected area of surface A_1 in the direction of A_2 and is

$$A_p(\Lambda) = A_1 f(\Lambda)$$

where to a viewer at dA_2, the area distribution $f(\Lambda)$ of surface A_1 is defined in the interval $-\pi$ to π by

$$\left.\begin{aligned} f(\Lambda) &= 0 \qquad \left(-\pi \leqq \Lambda \leqq -\frac{\pi}{2}\right) \\ f(\Lambda) &= \cos\Lambda \qquad \left(-\frac{\pi}{2} < \Lambda < \frac{\pi}{2}\right) \\ f(\Lambda) &= 0 \qquad \left(\frac{\pi}{2} \leqq \Lambda \leqq \pi\right) \end{aligned}\right\} \tag{7}$$

By use of the spherical coordinate system of figure 1, equation (6) can be expressed as

$$F_{12} = \frac{1}{\pi} \int_0^{2\pi} \int_0^{\alpha_L} f(\Lambda)\sin \alpha \, d\alpha \, d\varphi \tag{8}$$

As in reference 7, $f(\Lambda)$ can be expanded in a Fourier series:

$$f(\Lambda) = \sum_{N=0}^{\infty} a_N \cos N\Lambda \tag{9}$$

The series is rapidly convergent and represents $f(\Lambda)$ to a high degree of accuracy (within 3 percent) when truncated at $N = 6$. Thus,

$$f(\Lambda) = \frac{1}{\pi} + \frac{1}{2} \cos \Lambda + \frac{2}{3\pi} \cos 2\Lambda - \frac{2}{15\pi} \cos 4\Lambda + \frac{2}{35\pi} \cos 6\Lambda \tag{10}$$

or equivalently

$$f(\Lambda) = \frac{1}{7\pi} + \frac{1}{2} \cos \Lambda + \frac{24}{7\pi} \cos^2\Lambda - \frac{80}{21\pi} \cos^4\Lambda + \frac{64}{35\pi} \cos^6\Lambda \tag{11}$$

From figure 1, spherical trigonometry gives the relation

$$\cos \Lambda = \cos \lambda \cos \alpha + \sin \lambda \sin \alpha \cos \varphi \tag{12}$$

Substitution of equations (11) and (12) into equation (8) and performing the indicated integration gives

$$F_{12}\left(\lambda,\alpha_L\right) = B_0 + B_1 \cos \lambda + B_2 \cos^2\lambda + B_3 \cos^4\lambda + B_4 \cos^6\lambda \tag{13}$$

where

$$
\left.
\begin{aligned}
B_0 &= \frac{2}{7\pi}\left(\frac{577}{105} - 7\cos\alpha_L + \frac{4}{3}\cos^3\alpha_L - \frac{2}{5}\cos^5\alpha_L + \frac{4}{7}\cos^7\alpha_L\right) \\
B_1 &= \frac{1}{2}\sin^2\alpha_L \\
B_2 &= \frac{8}{7\pi}\left(\cos\alpha_L - 2\cos^3\alpha_L + 4\cos^5\alpha_L - 3\cos^7\alpha_L\right) \\
B_3 &= \frac{4}{7\pi}\left(-\cos\alpha_L + \frac{40}{3}\cos^3\alpha_L - \frac{91}{3}\cos^5\alpha_L + 18\cos^7\alpha_L\right) \\
B_4 &= \frac{8}{35\pi}\left(5\cos\alpha_L - 35\cos^3\alpha_L + 63\cos^5\alpha_L - 33\cos^7\alpha_L\right) \\
\alpha_L &= \sin^{-1}\left(\frac{R}{H}\right) \\
H &= \frac{\left(h_p + R\right)(1 + \epsilon)}{1 + \epsilon\cos\eta} \\
h &= H - R
\end{aligned}
\right\} \qquad (14)
$$

Equation (13) expresses the instantaneous geometric shape factor between a planar surface and a spherical planet as a function of the attitude angle λ which is defined for an arbitrary orientation in figure 1, and orbit altitude h. Results of equation (13) are shown graphically in figure 2. The parameters B_0, B_1, B_2, B_3, and B_4 are tabulated for h/R ratios of 0.001 to 10.0 in table I. For a solar-oriented vehicle, λ in terms of orbit parameters (see appendix for derivation) is defined as

$$
\begin{aligned}
\cos\lambda = -\Big\{&\cos\gamma\left[\left(A_1\cos\xi - A_2\sin\xi\right)\cos\delta + A_3\sin\delta\right] \\
&+ \sin\gamma\left[\left(A_4\cos\xi - A_5\sin\xi\right)\cos\delta + A_6\sin\delta\right]\Big\}
\end{aligned} \qquad (15)
$$

where

$$A_1 = \cos \Omega \cos \beta + \cos i \sin \Omega \sin \beta$$

$$A_2 = \cos \nu \sin \beta \sin i + \sin \nu(\sin \beta \cos i \cos \Omega - \sin \Omega \cos \beta)$$

$$A_3 = \cos \nu(\sin \beta \cos i \cos \Omega - \sin \Omega \cos \beta) - \sin \nu \sin \beta \sin i$$

$$A_4 = -\cos \Omega \cos I \sin \beta + \cos i \sin \Omega \cos I \cos \beta + \sin i \sin \Omega \sin I$$

$$A_5 = \cos \nu(\cos I \cos \beta \sin i - \sin I \cos i) + \sin \nu(\sin \Omega \cos I \sin \beta + \sin I \sin i \cos \Omega + \cos I \cos \beta \cos i \cos \Omega)$$

$$A_6 = \cos \nu(\sin \Omega \cos I \sin \beta + \cos I \cos \beta \cos i \cos \Omega + \sin I \sin i \cos \Omega) + \sin \nu(\sin I \cos i - \cos I \cos \beta \sin i)$$

Bodies of revolution.- Geometric shape factors are determined for instantaneous (nonspinning) and spinning bodies of revolution.

Instantaneous geometric shape factor: If one considers a convex surface to be composed of an infinite number of planar elements, the instantaneous geometric shape factor for a right circular conical frustum is given by

$$F\left(\delta,\theta,\alpha_L\right) = \frac{1}{2\pi} \int_0^{2\pi} F\left(\lambda,\alpha_L\right) d\xi \tag{16}$$

where, from figure 3, spherical trigonometry gives

$$\cos \lambda = \sin \delta \cos \theta + \cos \delta \sin \theta \cos \xi \tag{17}$$

Substituting equations (13) and (17) into equation (16) gives upon integration

$$F\left(\delta,\theta,\alpha_L\right) = B_0 + B_1(C) + B_2\left(C^2 + \frac{D^2}{2}\right) + B_3\left(C^4 + 3C^2D^2 + \frac{3}{8} D^4\right) + B_4\left(C^6 + \frac{15}{2} C^4D^2 + \frac{45}{8} C^2D^4 + \frac{5}{16} D^6\right) \tag{18}$$

where

$$C = \sin \delta \cos \theta$$

$$D = \cos \delta \sin \theta$$

Equation (18) expresses the instantaneous geometric shape factor between the cone and a spherical planet as a function of the semiapex angle δ, the attitude angle θ which is defined for an arbitrary orientation in figure 3, and orbit altitude h. The attitude angle θ in terms of orbit parameters for a solar-oriented vehicle is defined in the following equation (derived in the appendix):

$$\begin{aligned}\cos\theta = -\Big\{&\cos\gamma\left[\cos\nu(\cos i\cos\Omega\sin\beta - \sin\Omega\cos\beta) - \sin\nu(\sin i\sin\beta)\right] \\ &+ \sin\gamma\left[\cos\nu(\sin\Omega\cos I\sin\beta + \cos i\cos\Omega\cos I\cos\beta\right. \\ &\left.+ \sin i\cos\Omega\sin I) + \sin\nu(\cos i\sin I - \sin i\cos I\cos\beta)\right]\Big\}\end{aligned} \tag{19}$$

Results of equation (18) are shown graphically in figures 4, 5, and 6. Setting $\delta = 0^\circ$ or 90° in equation (18) gives the geometric shape factor for a cylinder and a planar surface, respectively. For $\delta = 0^\circ$, the geometric shape factor for a cylindrical configuration is

$$F\left(0,\theta,\alpha_L\right) = B_0 + \frac{B_2}{2}\sin^2\theta + \frac{3B_3}{8}\sin^4\theta + \frac{5B_4}{16}\sin^6\theta \tag{20}$$

For $\delta = 90^\circ$, equation (18) reduces to equation (13) with $\theta \equiv \lambda$. Equation (18) also gives the geometric shape for a spinning planar surface where the axis of symmetry is the angular momentum vector and the angle $90^\circ - \delta$ becomes the attitude angle of the planar surface with respect to this vector.

For a general convex body of revolution, the instantaneous geometric shape factor is given by

$$F\left(\theta,\alpha_L\right)_{gen} = \frac{\int_A F\left(\lambda,\alpha_L\right)dA}{\int_A dA} \tag{21}$$

where $F\left(\lambda,\alpha_L\right)$ is the instantaneous geometric shape factor to an infinitesimal planar surface element and dA is the surface element which must be appropriately described for the general configuration.

It follows that the instantaneous geometric shape factor for a hemispherical configuration can be expressed as

$$F\left(\theta,\alpha_L\right) = \frac{1}{2\pi}\int_0^{\pi/2}\int_0^{2\pi} F\left(\lambda,\alpha_L\right)\cos\delta\, d\xi\, d\delta \tag{22}$$

or equivalently

$$F\left(\theta,\alpha_L\right) = \int_0^{\pi/2} F\left(\delta,\theta,\alpha_L\right)\cos\,\delta\,d\delta \tag{23}$$

Substituting equation (18) into equation (23) and integrating gives

$$F\left(\theta,\alpha_L\right) = B_0 + \frac{B_1}{2}\cos\,\theta + \frac{B_2}{3} + \frac{B_3}{5} + \frac{B_4}{7} \tag{24}$$

Results of equation (24) are shown graphically in figure 7.

The geometric shape factor for a spherical configuration is obtained by setting $\theta = 90^\circ$ in equation (24) which gives

$$F\left(90,\alpha_L\right) = B_0 + \frac{B_2}{3} + \frac{B_3}{5} + \frac{B_4}{7} \tag{25}$$

Results of equation (25) are shown graphically in figure 8.

Spinning geometric shape factor: If the spacecraft is spinning with the angular momentum vector normal to the principal axis as shown in figure 9, then

$$\cos\,\theta = \sin\,\Phi\,\cos\,\nu \tag{26}$$

If it is assumed that the spin rate is sufficiently fast (that is, the ratio of orbit to spacecraft angular velocity is small), the geometric shape factor for a cone averaged over a spin cycle is defined as

$$F\left(\delta,\Phi,\alpha_L\right) = \frac{1}{2\pi}\int_0^{2\pi} F\left(\delta,\theta,\alpha_L\right)d\nu \tag{27}$$

Substituting equations (18) and (26) into equation (27) gives upon integration

$$\begin{aligned} F\left(\delta,\Phi,\alpha_L\right) = B_0 &+ \frac{B_2}{2}\left(E^2 + G^2 + \frac{K^2}{2}\right) \\ &+ \frac{3B_3}{8}\left(E^4 + 4G^2E^2 + K^2E^2 + 3G^2K^2 + G^4 + \frac{3}{8}K^4\right) \\ &+ \frac{5B_4}{16}\left(E^6 + 9G^2E^4 + \frac{3}{2}E^4K^2 + 9E^2G^4\right. \\ &\left. + \frac{27}{2}G^2K^2E^2 + \frac{9}{8}E^2K^4 + G^6 + \frac{15}{2}G^4K^2 + \frac{45}{8}G^2K^4 + \frac{5}{16}K^6\right) \end{aligned} \tag{28}$$

where

$$E = \cos \delta$$

$$G = \sin \delta \sin \Phi$$

$$K^2 = -\cos^2\delta \sin^2\Phi$$

Equation (28) expresses the geometric shape factor between a spinning cone and a spherical planet as a function of the semiapex angle δ, the attitude angle Φ which is defined for an arbitrary orientation in figure 9, and the orbit altitude h. Results of equation (28) are shown graphically in figures 10, 11, and 12. Setting $\delta = 0^\circ$ gives

$$F\left(0,\Phi,\alpha_L\right) = B_0 + \frac{B_2}{2}\left(1 - \frac{1}{2}\sin^2\Phi\right) + \frac{3B_3}{8}\left(\cos^2\Phi + \frac{3}{8}\sin^4\Phi\right)$$

$$+ \frac{5B_4}{16}\left(1 - \frac{3}{2}\sin^2\Phi + \frac{9}{8}\sin^4\Phi - \frac{5}{16}\sin^6\Phi\right) \tag{29}$$

which is the geometric shape factor for a cylindrical configuration. The attitude angle Φ appearing in equations (28) and (29) is defined (and derived in the appendix) in terms of orbit parameters for a solar-oriented spacecraft as

$$\cos \Phi = -\Big[\cos \gamma(\cos \beta \cos \Omega + \sin \beta \cos i \sin \Omega)$$

$$+ \sin \gamma(\cos I \cos \beta \cos i \sin \Omega - \cos I \sin \beta \cos \Omega$$

$$+ \sin I \sin i \sin \Omega)\Big] \tag{30}$$

Example problem.- As an example problem, consider the manned orbital research laboratory concept as shown in the spinning and nonspinning modes of operation in figures 13 and 14, respectively. It is required to calculate the external radiant heat flux incident upon several points on the surface of this vehicle as it orbits the earth for both modes of operation. Also, let the vehicle be solar oriented (that is, the axis of symmetry is normal to an orientation vector which is pointed at the sun) and let the sun and ascending orbit node be located at the vernal equinox and let the orbit plane be coincident with the ecliptic plane. Thus, for a circular 200-nautical-mile orbit

$\Omega = 0^\circ$	$\gamma_p = 0^\circ$
$\beta = 0^\circ$	$C_s = 443$ Btu/hr-ft^2
$I = 23.5^\circ$	$R = 3435.058$ nautical miles
$i = 23.5^\circ$	$a = 0.36$
$\epsilon = 0$	$h = 200$ nautical miles

The points of interest are the locations of antennae on the cylindrical section of the vehicle and the antennae are positioned with respect to the orientation vector (pointed at the sun) by $\xi = 45^\circ$ and $\xi = 315^\circ$. (See fig. 3.)

Instantaneous (nonspinning) shape factor: The instantaneous geometric shape factor is given by equation (13) where the attitude angle λ is defined by equation (15). For this mode of operation, assume the axis of symmetry of the vehicle to be inclined normal to the ecliptic plane (that is, $\nu = 90^\circ$), and setting $\delta = 0^\circ$ (for a cylinder) gives

$$\cos \lambda = \sin \xi \sin \gamma - \cos \xi \cos \gamma$$

For this case, equation (30) reduces to

$$\cos \Phi = -\cos \gamma = -\cos \eta_s$$

Substitution of this equation into equations (1) and (4) gives the planetary-thermal and planetary-reflected solar radiation incident to $\xi = 45^\circ$ and $\xi = 315^\circ$ for the nonspinning mode of operation shown in figures 15 and 16, respectively.

Spinning shape factor: The geometric shape factor is given by equation (18) where $\delta = 90^\circ - \xi$ and where for this case, the attitude angle θ defined by equation (19) is

$$\theta = 180^\circ - \eta_s = 180^\circ - \gamma$$

Substitution of this equation into equations (1) and (4) gives the planetary-thermal and planetary-reflected solar radiation incident to $\xi = 45^\circ$ and $\xi = 315^\circ$ for the spinning mode of operation as shown in figures 15 and 16, respectively.

Solar radiation: For $|\xi| < 90^\circ$, incident solar radiation is given by

$$q_s = C_s A \cos \xi$$

in sunlight and by

$$q_s = 0$$

in shadow. Shadow entrance and exit occur when, from reference 7,

$$\cos \eta_s = -\cos \alpha_L$$

where from equation (14)

$$\alpha_L = \sin^{-1}\left(\frac{R}{H}\right) = \sin^{-1}\left(\frac{R}{R + h}\right)$$

Solution of these equations gives

$$\eta_{s_{ent}} = 109.1^\circ$$

$$\eta_{s_{exit}} = 250.9^\circ$$

For the example, the incident solar radiation to $\xi = 45^\circ$ and $\xi = 315^\circ$ for both modes of operation is

$$\frac{q_s}{A} = 443(0.70711) = 313.25 \text{ Btu/hr-ft}^2 \qquad (-109.1^\circ < \gamma < 109.1^\circ)$$

$$\frac{q_s}{A} = 0 \qquad (109.1^\circ \leqq \gamma \leqq 250.9^\circ)$$

where $\gamma = \eta_s$.

RESULTS AND DISCUSSION

The geometric shape factors calculated by the approximate expressions given in this report are compared with graphical and tabulated data given in references 3, 5, and 8 for several spacecraft configurations in table II. The accuracy of the approximate solutions, as demonstrated in table II, is sufficient for most engineering applications because of the uncertainty regarding the variation of local planet surface optical properties from the assumed mean values.

Graphical results for the nonspinning planar surface (eq. (13)) are given in figure 2. The geometric shape factor for a spinning planar surface is determined from equation (18) and is plotted in figures 4, 5, and 6 for nonspinning cones with the appropriate semiapex angle δ. From equation (28), the results for spinning cones having the angular momentum vector normal to the axis of symmetry are shown graphically in figures 10, 11, and 12. The geometric shape factors for cylindrical bodies are found by setting $\delta = 0^\circ$ in equations (18) and (28). Results for hemispherical configurations (eq. (24)) and

spherical configurations (eq. (25)) are shown graphically in figures 7 and 8, respectively.

Equations (1) and (4) give the planetary-thermal and planetary-reflected solar radiant heat energy incident upon an orbiting spacecraft. If the spacecraft has solar orientation, the incident radiant heat energy at any point in orbit can be found for any desired time after orbit injection with the aid of the orbit geometry and the equations presented in the appendix.

The radiant heat energy incident upon configurations not presented in this report may be found by approximating the vehicle surface by planar elements.

If it is desired to determine the peripheral variation of radiant heat energy upon the configurations presented in this report, the appropriate geometric shape factor expression can be integrated between the desired peripheral positions, or the configuration may be approximated by planar surface elements.

CONCLUDING REMARKS

Truncated series expressions for the geometric shape factors for planetary-thermal and planetary-reflected solar radiation incident upon arbitrarily oriented spinning and nonspinning spacecraft are derived and discussed. Results indicate good agreement between the approximate closed form solutions of this report and existing computer solutions found in the literature.

The results of this study are of value in the thermal design of any orbiting spacecraft, spinning or nonspinning, since they can be used to predict the approximate radiant heat flux incident to the vehicle without the use of computers, and thus assist in the design of temperature control systems.

The radiant heat energy incident upon configurations not presented in this report may be found by approximating the vehicle surface by planar elements.

Langley Research Center,
National Aeronautics and Space Administration,
Langley Station, Hampton, Va., March 2, 1965.

APPENDIX

DERIVATION OF ATTITUDE ANGLES FOR A SPACECRAFT HAVING SOLAR ORIENTATION

The attitude angles λ, θ, and Φ defined in terms of orbit parameters for a vehicle having solar orientation are found by considering a nonrotating spherical planet with a fixed right-hand orthogonal coordinate system X, Y, and Z, with the Z-axis alined with the planet's axis of rotation (North Pole) and the X-axis alined with the intersections of the equatorial and ecliptic planes (vernal equinox). (See sketch (a).)

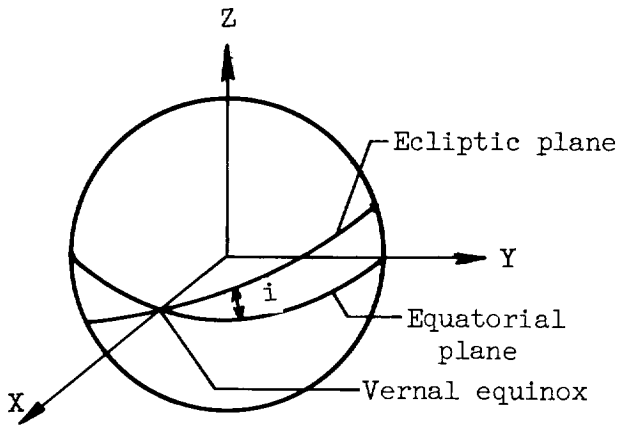

Sketch (a)

The position of a spacecraft relative to the fixed coordinate system is determined by considering a coordinate system X', Y', and Z' in the plane of the orbit having the Z'-axis perpendicular to the orbit plane and the X'-axis alined with the spacecraft's position as shown in sketch (b).

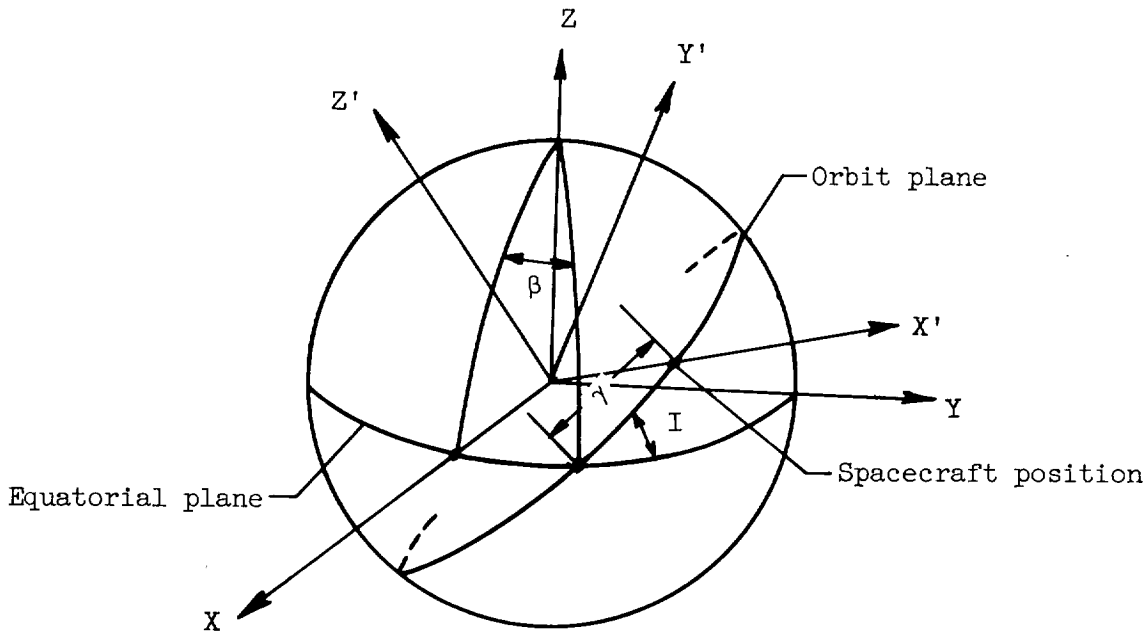

Sketch (b)

APPENDIX

Let i, j, and k represent unit vectors in the X, Y, and Z directions and i', j', and k' unit vectors in the X', Y', and Z' directions. The unit vectors i', j', and k' are defined by

$$\begin{Bmatrix} i' \\ j' \\ k' \end{Bmatrix} = M(\gamma)\, M(I)\, M(\beta) \begin{Bmatrix} i \\ j \\ k \end{Bmatrix}$$

where

$$M(\gamma) = \begin{bmatrix} \cos\gamma & \sin\gamma & 0 \\ -\sin\gamma & \cos\gamma & 0 \\ 0 & 0 & 1 \end{bmatrix}$$

$$M(I) = \begin{bmatrix} 1 & 0 & 0 \\ 0 & \cos I & \sin I \\ 0 & -\sin I & \cos I \end{bmatrix}$$

$$M(\beta) = \begin{bmatrix} \cos\beta & \sin\beta & 0 \\ -\sin\beta & \cos\beta & 0 \\ 0 & 0 & 1 \end{bmatrix}$$

Matrix multiplication gives

$$\begin{Bmatrix} i' \\ j' \\ k' \end{Bmatrix} = \begin{bmatrix} \cos\gamma\cos\beta - \sin\gamma\cos I\sin\beta & \cos\gamma\sin\beta + \sin\gamma\cos I\cos\beta & \sin\gamma\sin I \\ -\sin\gamma\cos\beta - \cos\gamma\cos I\sin\beta & -\sin\gamma\sin\beta + \cos\gamma\cos I\cos\beta & \cos\gamma\sin I \\ \sin I\sin\beta & -\sin I\cos\beta & \cos I \end{bmatrix} \begin{Bmatrix} i \\ j \\ k \end{Bmatrix}$$

The position of the sun relative to the fixed coordinate system is determined by considering a coordinate system X", Y", and Z" in the plane of the ecliptic having the Z"-axis perpendicular to the ecliptic plane and the X"-axis alined with the sun as shown in sketch (c).

APPENDIX

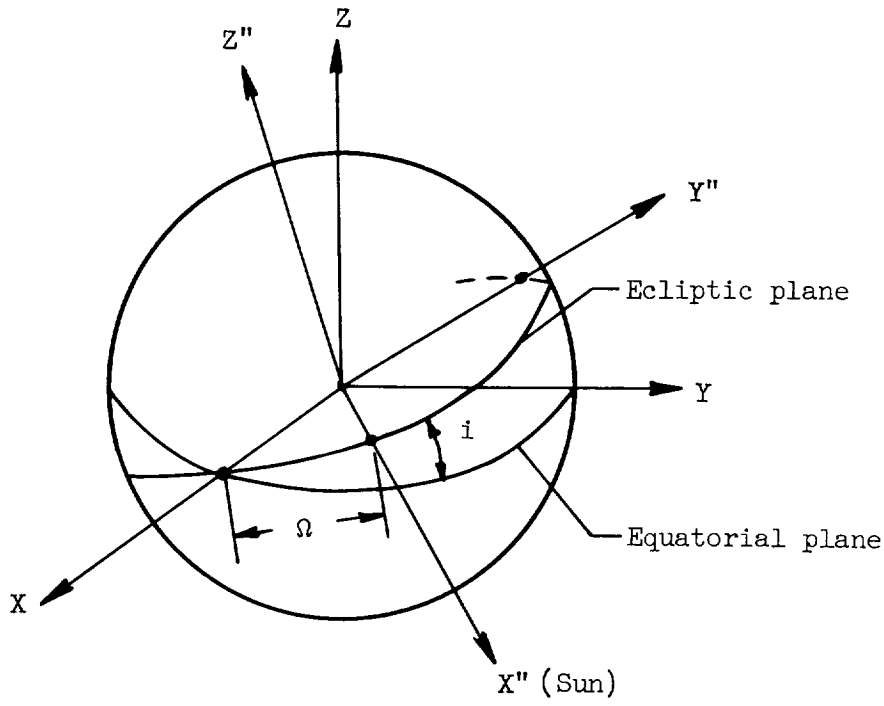

Sketch (c)

Unit vectors in the X", Y", and Z" coordinate system are given by

$$\begin{Bmatrix} i'' \\ j'' \\ k'' \end{Bmatrix} = M(\Omega)\, M(i) \begin{Bmatrix} i \\ j \\ k \end{Bmatrix}$$

where

$$M(\Omega) = \begin{bmatrix} \cos\Omega & \sin\Omega & 0 \\ -\sin\Omega & \cos\Omega & 0 \\ 0 & 0 & 1 \end{bmatrix}$$

$$M(i) = \begin{bmatrix} 1 & 0 & 0 \\ 0 & \cos i & \sin i \\ 0 & -\sin i & \cos i \end{bmatrix}$$

Therefore,

$$\begin{Bmatrix} i'' \\ j'' \\ k'' \end{Bmatrix} = \begin{bmatrix} \cos\Omega & \cos i \sin\Omega & \sin i \sin\Omega \\ -\sin\Omega & \cos i \cos\Omega & \sin i \cos\Omega \\ 0 & -\sin i & \cos i \end{bmatrix} \begin{Bmatrix} i \\ j \\ k \end{Bmatrix}$$

If the spacecraft is rotated about the solar unit vector i" through the angle ν, the unit vectors in a sun-oriented vehicle coordinate system X''', Y''', and Z''' are defined by

$$\begin{Bmatrix} i''' \\ j''' \\ k''' \end{Bmatrix} = M(\nu) \begin{Bmatrix} i'' \\ j'' \\ k'' \end{Bmatrix}$$

where

$$M(\nu) = \begin{bmatrix} 1 & 0 & 0 \\ 0 & \cos\nu & \sin\nu \\ 0 & -\sin\nu & \cos\nu \end{bmatrix}$$

Then i''', j''', and k''' are defined in terms of the fixed coordinate system by the transformation

$$\begin{Bmatrix} i''' \\ j''' \\ k''' \end{Bmatrix} = M(\nu)\, M(\Omega)\, M(i) \begin{Bmatrix} i \\ j \\ k \end{Bmatrix}$$

whereby matrix multiplication gives

$$\begin{Bmatrix} i''' \\ j''' \\ k''' \end{Bmatrix} = \begin{bmatrix} \cos\Omega & \cos i \sin\Omega & \sin i \sin\Omega \\ -\cos\nu \sin\Omega & \cos\nu \cos i \cos\Omega - \sin i \sin\nu & \cos\nu \sin i \cos\Omega + \sin\nu \cos i \\ \sin\nu \sin\Omega & -\sin\nu \cos i \cos\Omega - \cos\nu \sin i & -\sin\nu \sin i \cos\Omega + \cos\nu \cos i \end{bmatrix} \begin{Bmatrix} i \\ j \\ k \end{Bmatrix}$$

APPENDIX

Let e_1, e_2, and e_3 be unit vectors in the X_1, X_2, and X_3 directions of the right-hand orthogonal vehicle coordinate system shown in figure 3, and then the unit vector normal to a planar surface element in this system is given by

$$\bar{N} = e_1 \cos\delta \cos\xi + e_2 \sin\delta + e_3 \cos\delta \sin\xi$$

For a solar-oriented vehicle, if e_1 is selected as the orientation unit vector and e_2 as the axis of symmetry for the vehicle configuration, then

$$e_1 = i'''$$

$$e_2 = j'''$$

$$e_3 = k'''$$

and the normal vector becomes

$$\bar{N} = i''' \cos\delta \cos\xi + j''' \sin\delta - k''' \cos\delta \sin\xi \qquad (A1)$$

For an arbitrary solar-oriented spacecraft, the attitude angles λ, θ, and Φ can then be defined by

$$\cos\lambda = -(\bar{N} \cdot i')$$

$$\cos\theta = -(j''' \cdot i')$$

$$\cos\Phi = -(i''' \cdot i')$$

Performing the indicated mathematical operation yields

$$\cos\lambda = -\left\{\cos\gamma\left[\left(A_1 \cos\xi - A_2 \sin\xi\right)\cos\delta + A_3 \sin\delta\right]\right.$$
$$\left. + \sin\gamma\left[\left(A_4 \cos\xi - A_5 \sin\xi\right)\cos\delta + A_6 \sin\delta\right]\right\} \qquad (A2)$$

where

$$A_1 = \cos \Omega \cos \beta + \cos i \sin \Omega \sin \beta$$

$$A_2 = \cos \nu \sin \beta \sin i + \sin \nu(\sin \beta \cos i \cos \Omega - \sin \Omega \cos \beta)$$

$$A_3 = \cos \nu(\sin \beta \cos i \cos \Omega - \sin \Omega \cos \beta) - \sin \nu \sin \beta \sin i$$

$$A_4 = -\cos \Omega \cos I \sin \beta + \cos i \sin \Omega \cos I \cos \beta + \sin i \sin \Omega \sin I$$

$$A_5 = \cos \nu(\cos I \cos \beta \sin i - \sin I \cos i) + \sin \nu(\sin \Omega \cos I \sin \beta + \sin I \sin i \cos \Omega + \cos I \cos \beta \cos i \cos \Omega)$$

$$A_6 = \cos \nu(\sin \Omega \cos I \sin \beta + \cos I \cos \beta \cos i \cos \Omega + \sin I \sin i \cos \Omega) + \sin \nu(\sin I \cos i - \cos I \cos \beta \sin i)$$

and

$$\cos \theta = -\Big\{\cos \gamma\big[\cos \nu(\cos i \cos \Omega \sin \beta - \sin \Omega \cos \beta) - \sin \nu(\sin i \sin \beta)\big] + \sin \gamma\big[\cos \nu(\sin \Omega \cos I \sin \beta + \cos i \cos \Omega \cos I \cos \beta + \sin i \cos \Omega \sin I) + \sin \nu(\cos i \sin I - \sin i \cos I \cos \beta)\big]\Big\} \tag{A3}$$

$$\cos \Phi = -\big[\cos \gamma(\cos \beta \cos \Omega + \sin \beta \cos i \sin \Omega) + \sin \gamma(\cos I \cos \beta \cos i \sin \Omega - \cos I \sin \beta \cos \Omega + \sin I \sin i \sin \Omega)\big] \tag{A4}$$

For an elliptical orbit, the spacecraft position angle γ (measured from ascending orbit node) can be replaced for convenience in the previous attitude angle equations by the angle $\gamma_p + \eta$ where γ_p is the argument of the perigee (measured from ascending orbit node) and η is the spacecraft position angle measured from the orbit perigee. The orbit altitude, for this case, is given by equation (14) as a function of the perigee altitude h_p and orbit eccentricity ϵ. With this substitution $\cos \Phi$ becomes $-\cos \eta_s$.

REFERENCES

1. Swalley, Frank E.: Thermal Radiation Incident on an Earth Satellite. NASA TN D-1524, 1962.

2. Cunningham, Fred G.: Earth Reflected Solar Radiation Incident Upon an Arbitrary Oriented Spinning Flat Plate. NASA TN D-1842, 1963.

3. Cunningham, Fred G.: Power Input to a Small Flat Plate From a Diffusely Radiating Sphere With Application to Earth Satellites: The Spinning Plate. NASA TN D-1545, 1963.

4. Ballinger, J. C.; Elizalde, J. C.; and Christensen, E. H.: Thermal Environment of Interplanetary Space. [Preprint] 344B, Soc. Automotive Eng., 1961.

5. Christensen, E. H.: Radiation Geometric Factors Between Planets and Space Vehicles. Rept. No. AY62-0037 (Contract AF18(600)-1775), Convair Astronaut., Sept. 10, 1962.

6. Eckert, E. R. G. (with Pt. A and appendix by Robert M. Drake, Jr.): Heat and Mass Transfer. Second ed. of Introduction to the Transfer of Heat and Mass, McGraw-Hill Book Co., Inc., 1959.

7. Hastings, Earl C., Jr.; Turner, Richard E.; and Speegle, Katherine C.: Thermal Design of Explorer XIII Micrometeoroid Satellite. NASA TN D-1001, 1962.

8. Ballinger, John C.; and Christensen, Emmet H.: Environmental Control Study of Space Vehicles (Part II). Thermal Environment of Space - Supplement B. Tabular Presentation of Planetary Thermal and Planetary Albedo Radiation Incident to Space Vehicles. Rept. No. ERR-AN-016, Convair Astronaut., Jan. 20, 1961.

TABLE I.- PARAMETERS DEFINED BY EQUATION (14) TABULATED

FOR h/R RATIOS FROM 0.001 TO 10.0

h/R	B_0	B_1	B_2	B_3	B_4
0.001	0.47133	0.49900	0.01619	-0.00791	0.01603
.002	.45960	.49801	.02279	-.01088	.02234
.003	.45062	.49701	.02778	-.01295	.02695
.004	.44308	.49602	.03193	-.01453	.03066
.005	.43646	.49504	.03554	-.01578	.03377
.006	.43050	.49405	.03875	-.01678	.03644
.007	.42503	.49307	.04166	-.01758	.03877
.008	.41996	.49210	.04434	-.01822	.04082
.009	.41521	.49112	.04682	-.01873	.04264
.01	.41074	.49015	.04913	-.01912	.04427
.02	.37524	.48058	.06654	-.01889	.05353
.03	.34888	.47130	.07825	-.01443	.05565
.04	.32737	.46228	.08699	-.00794	.05403
.05	.30901	.45351	.09386	-.00045	.05023
.06	.29292	.44500	.09947	.00746	.04508
.07	.27858	.43672	.10416	.01541	.03915
.08	.26562	.42867	.10819	.02316	.03279
.09	.25382	.42084	.11170	.03054	.02626
.10	.24298	.41322	.11483	.03747	.01972
.20	.16729	.34722	.13609	.07596	-.03032
.30	.12301	.29586	.15017	.07118	-.04807
.40	.09396	.25510	.15976	.04693	-.04617
.50	.07374	.22222	.16514	.01785	-.03571
.60	.05912	.19531	.16691	-.00934	-.02279
.70	.04824	.17301	.16583	-.03220	-.01029
.80	.03996	.15432	.16268	-.05026	.00061
.90	.03353	.13850	.15810	-.06392	.00960
1.0	.02847	.12500	.15260	-.07384	.01674
2.0	.00849	.05556	.09456	-.08116	.03359
3.0	.00394	.03125	.05942	-.05787	.02588
4.0	.00227	.02000	.03999	-.04098	.01886
5.0	.00148	.01389	.02853	-.03001	.01400
6.0	.00105	.01020	.02130	-.02275	.01070
7.0	.00078	.00781	.01648	-.01777	.00840
8.0	.00060	.00617	.01312	-.01423	.00675
9.0	.00048	.00500	.01068	-.01164	.00553
10.0	.00040	.00413	.00886	-.00969	.00461

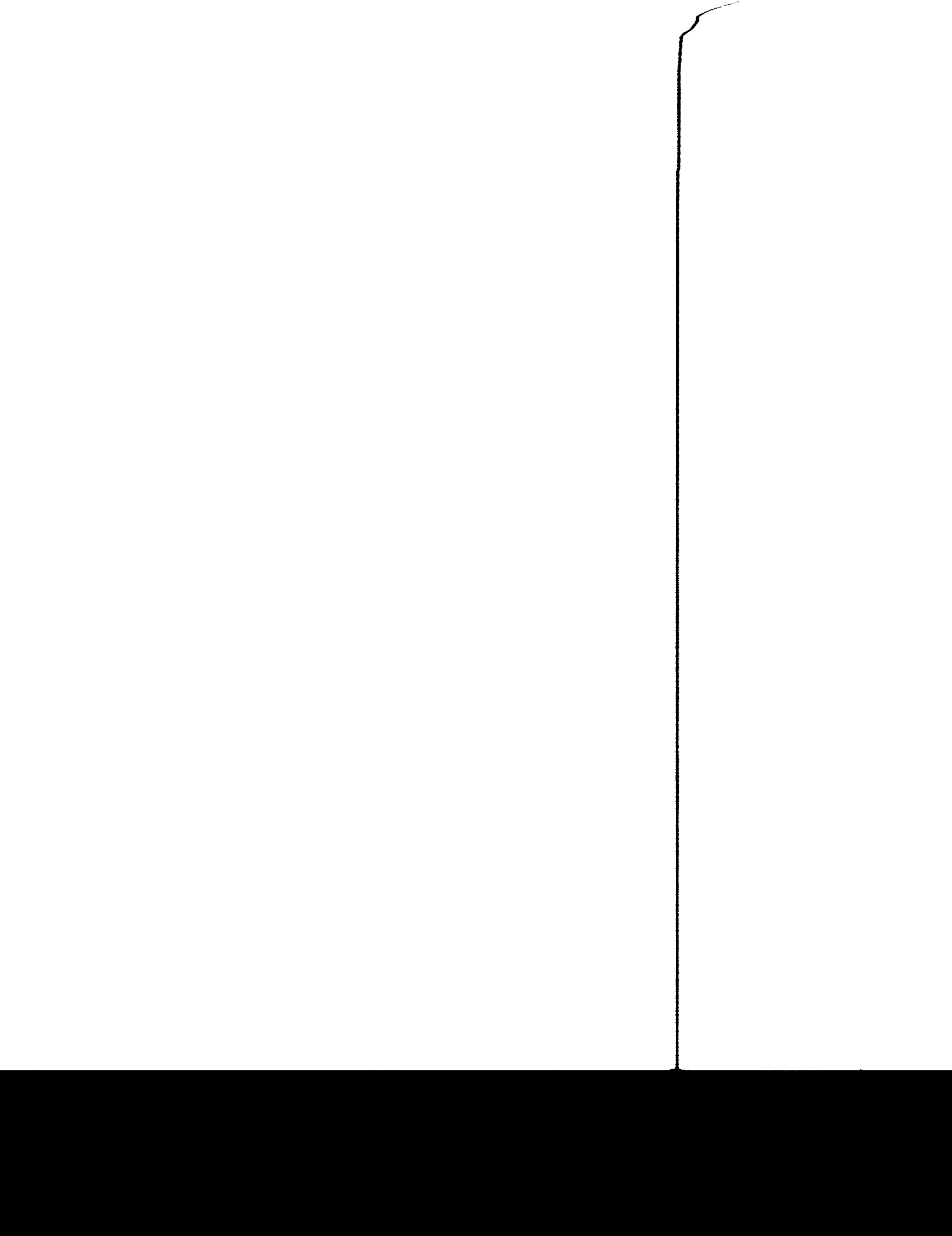

TABLE II.- COMPARISON OF RESULTS

Configuration	h/R	Attitude, deg	F (*)	F (**)	Reference
Nonspinning planar surface (eq. (13))	0.1164	$\lambda = 0$	0.8043	0.8020	8
	.1164	$\lambda = 60$	.4604	.4611	8
	.1164	$\lambda = 90$	.0593	.0598	8
	0.2911	$\lambda = 0$	0.6004	0.6000	8
	.2911	$\lambda = 60$	.3172	.3174	8
	.2911	$\lambda = 90$	.0173	.0172	8
Nonspinning body of revolution or spinning planar surface (eq. (18))	0.1164	$\delta = 0$, $\theta = 0$	0.2269	0.2267	5 and 8
	.1164	$\delta = 0$, $\theta = 30$	.2429	.2419	3
	.1164	$\delta = 0$, $\theta = 90$	.3071	.3054	5 and 8
	.1164	$\delta = 0$, $\theta = 90$	.3071	.3046	3
	.1164	$\delta = 60$, $\theta = 30$	.6219	.6182	3
	0.2911	$\delta = 0$, $\theta = 0$	0.1262	0.1262	5 and 8
	.2911	$\delta = 0$, $\theta = 30$	.1463	.1456	3
	.2911	$\delta = 0$, $\theta = 90$	.2131	.2126	5 and 8
	.2911	$\delta = 0$, $\theta = 90$	.2131	.2105	3
	.2911	$\delta = 60$, $\theta = 30$	.4544	.4569	3
Hemisphere (eq. (24))	0.1164	$\theta = 0$	0.4781	0.4768	5 and 8
	.1164	$\theta = 60$	.3778	.3850	5 and 8
	.1164	$\theta = 120$	.1772	.1860	5 and 8
	.1164	$\theta = 180$	.0769	.0788	5 and 8
	0.2911	$\theta = 0$	0.3336	0.3334	5 and 8
	.2911	$\theta = 60$	.2586	.2629	5 and 8
	.2911	$\theta = 120$	.1086	.1134	5 and 8
	.2911	$\theta = 180$	.0336	.0344	5 and 8
Sphere (eq. (25))	0.1164		0.2775	0.2778	8
	.2911		.1836	.1840	8
	.5000		.1272	.1274	5
	.7000		.0956	.0956	5

*Values calculated by methods of this report.
**Values taken from indicated reference.

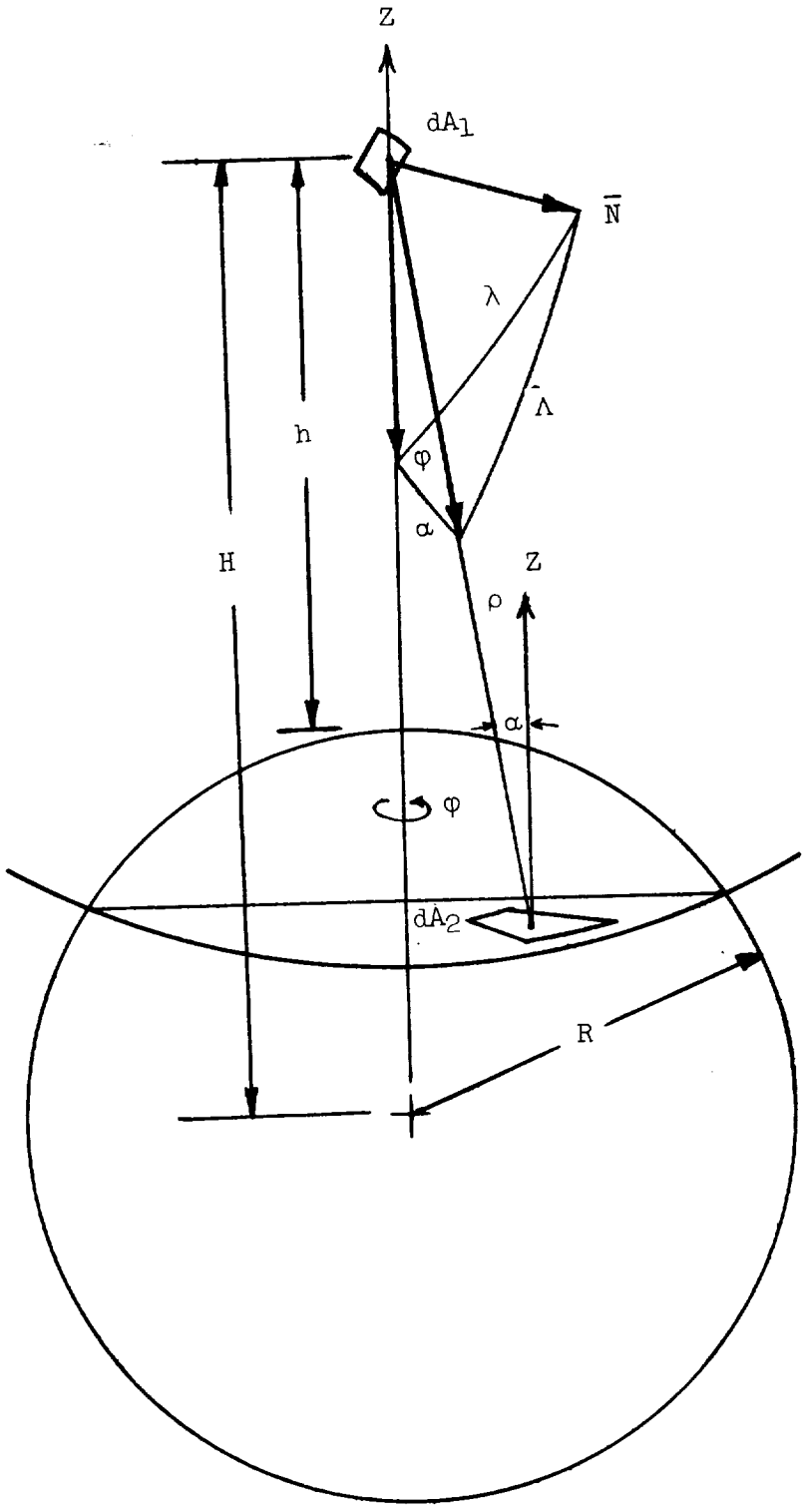

Figure 1.- Geometric-shape-factor geometry for planar surface.

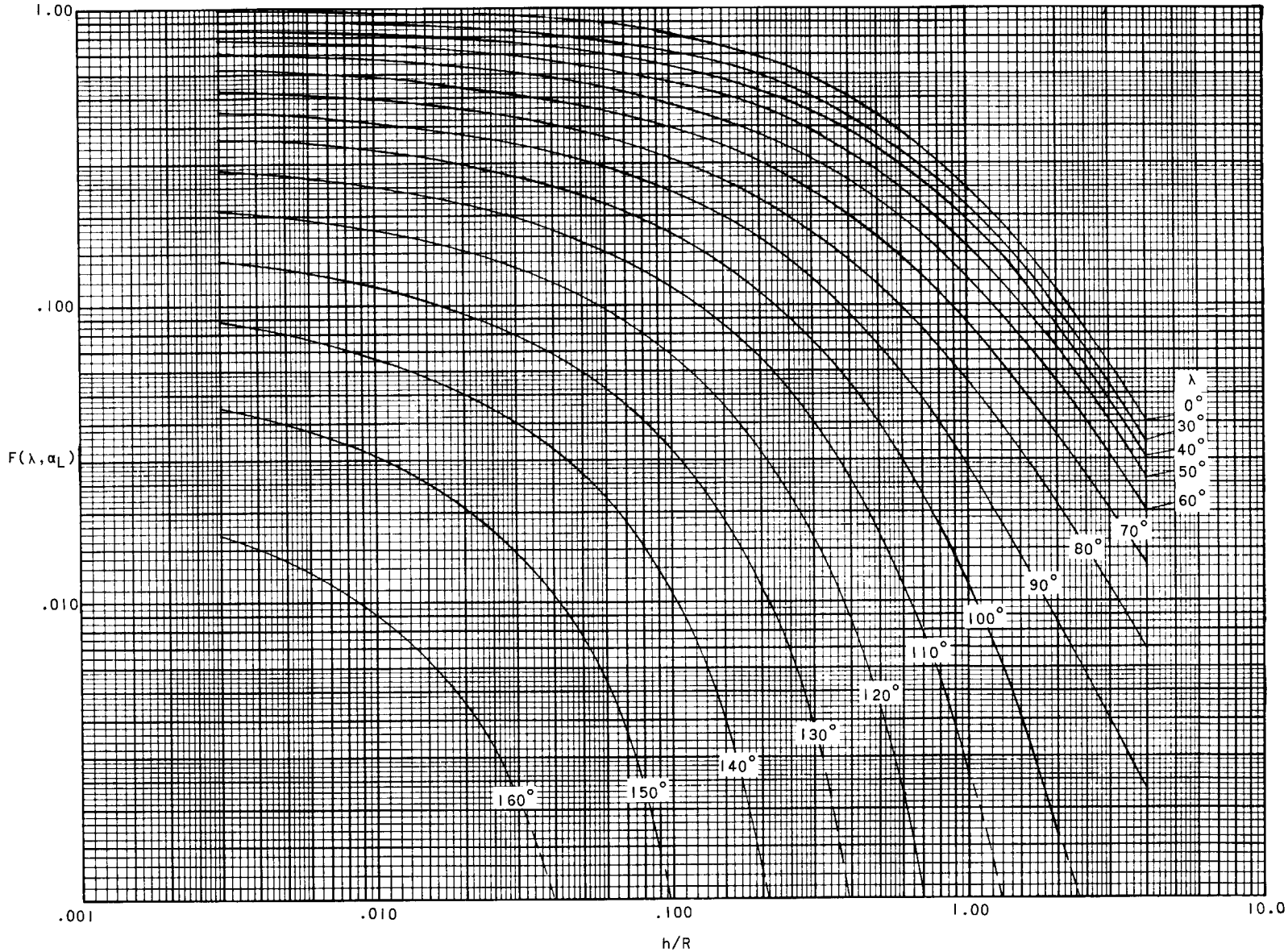

Figure 2.- Instantaneous geometric shape factor for a planar surface as a function of altitude and attitude.

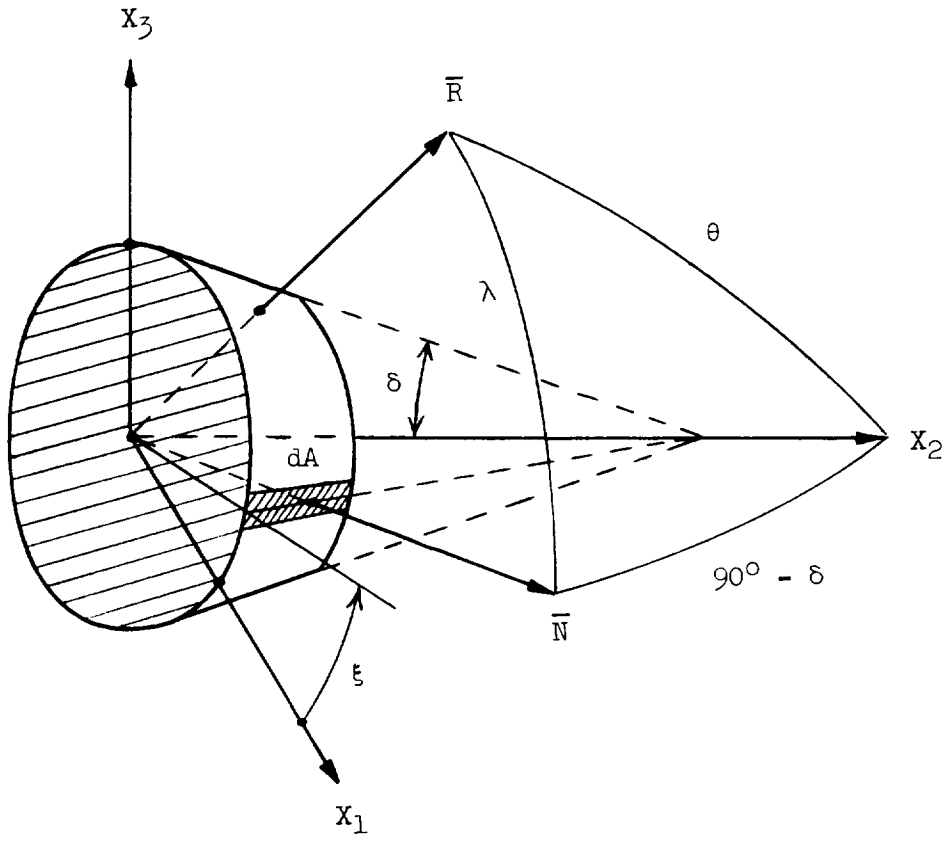

Figure 3.- Orientation of planar surface in vehicle coordinate system.

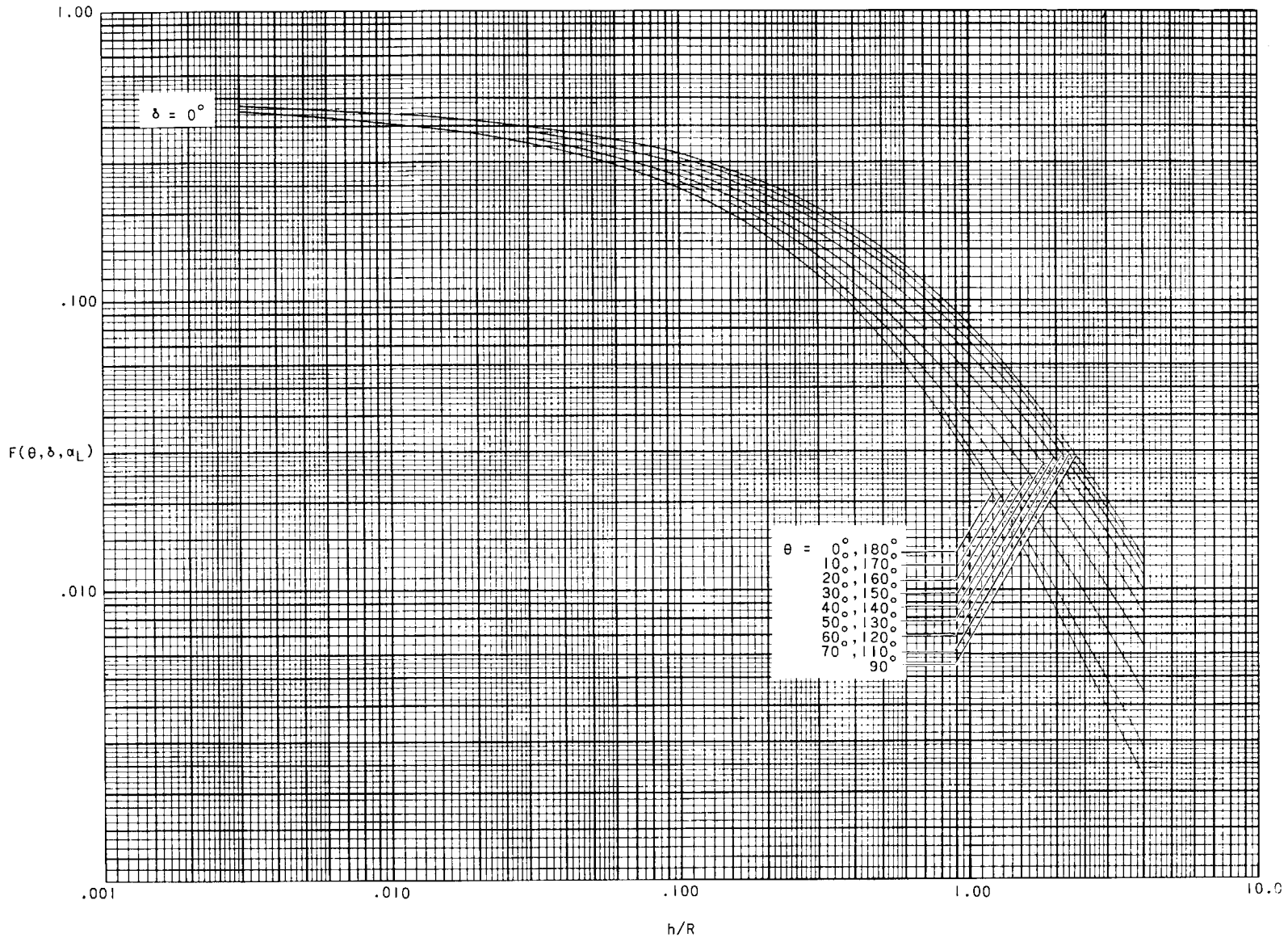

Figure 4.- Instantaneous geometric shape factor for a right circular cylinder ($\delta = 0^{o}$) as a function of altitude and attitude.

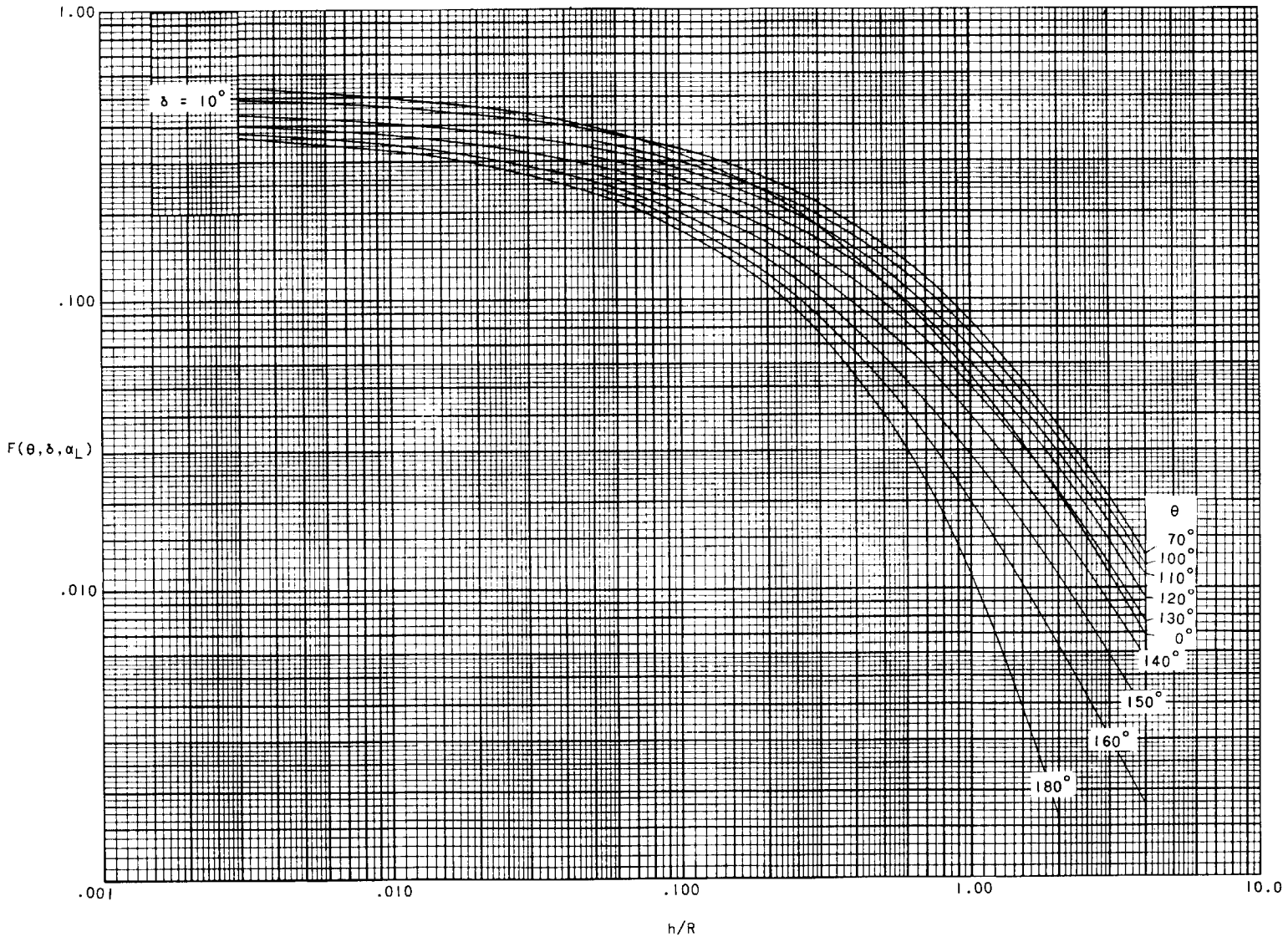

(a) $\delta = 10^{\circ}$.

Figure 5.- Instantaneous geometric shape factor for a cone as a function of altitude and attitude.

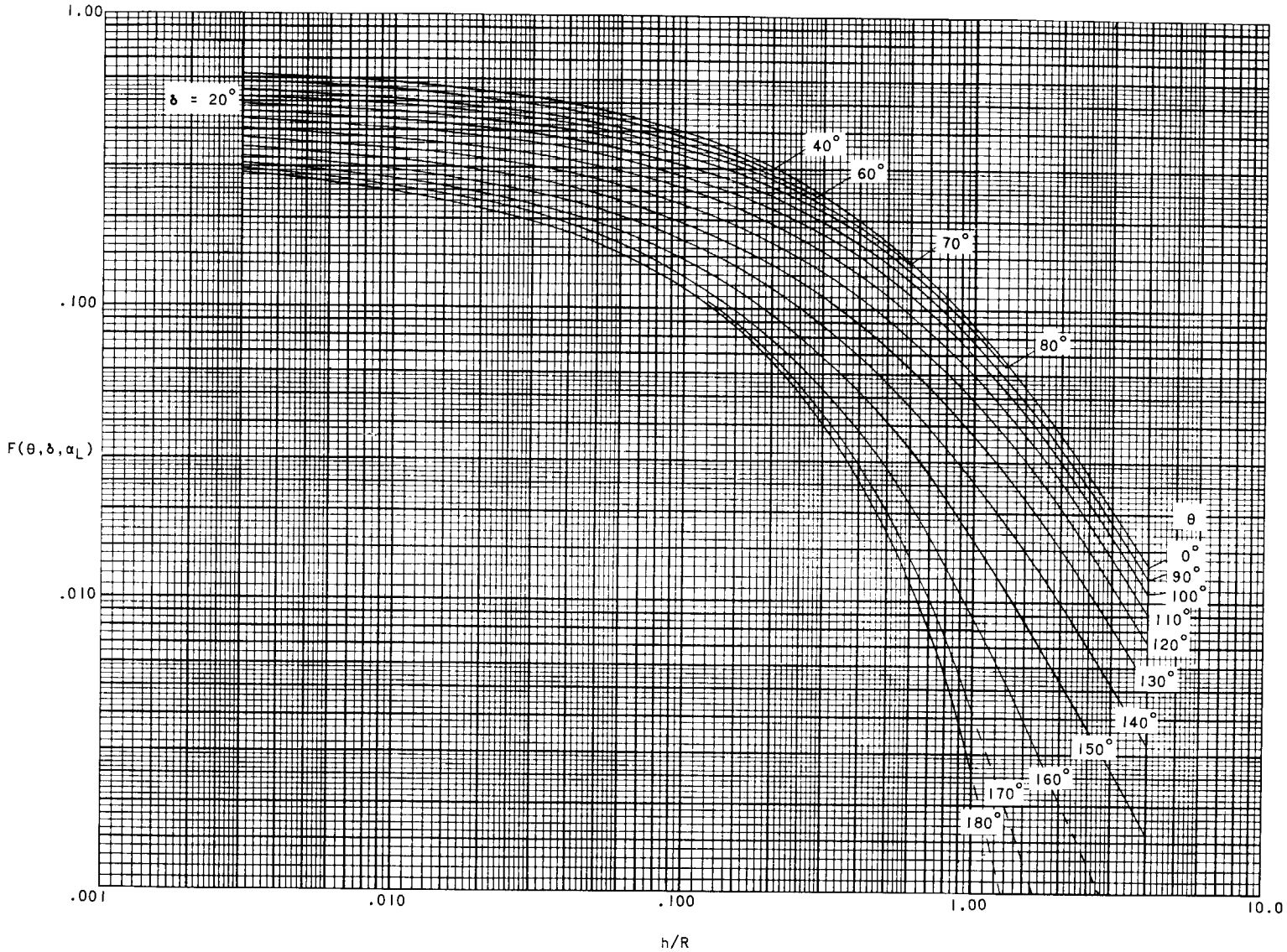

(b) $\delta = 20^{\circ}$.

Figure 5.- Continued.

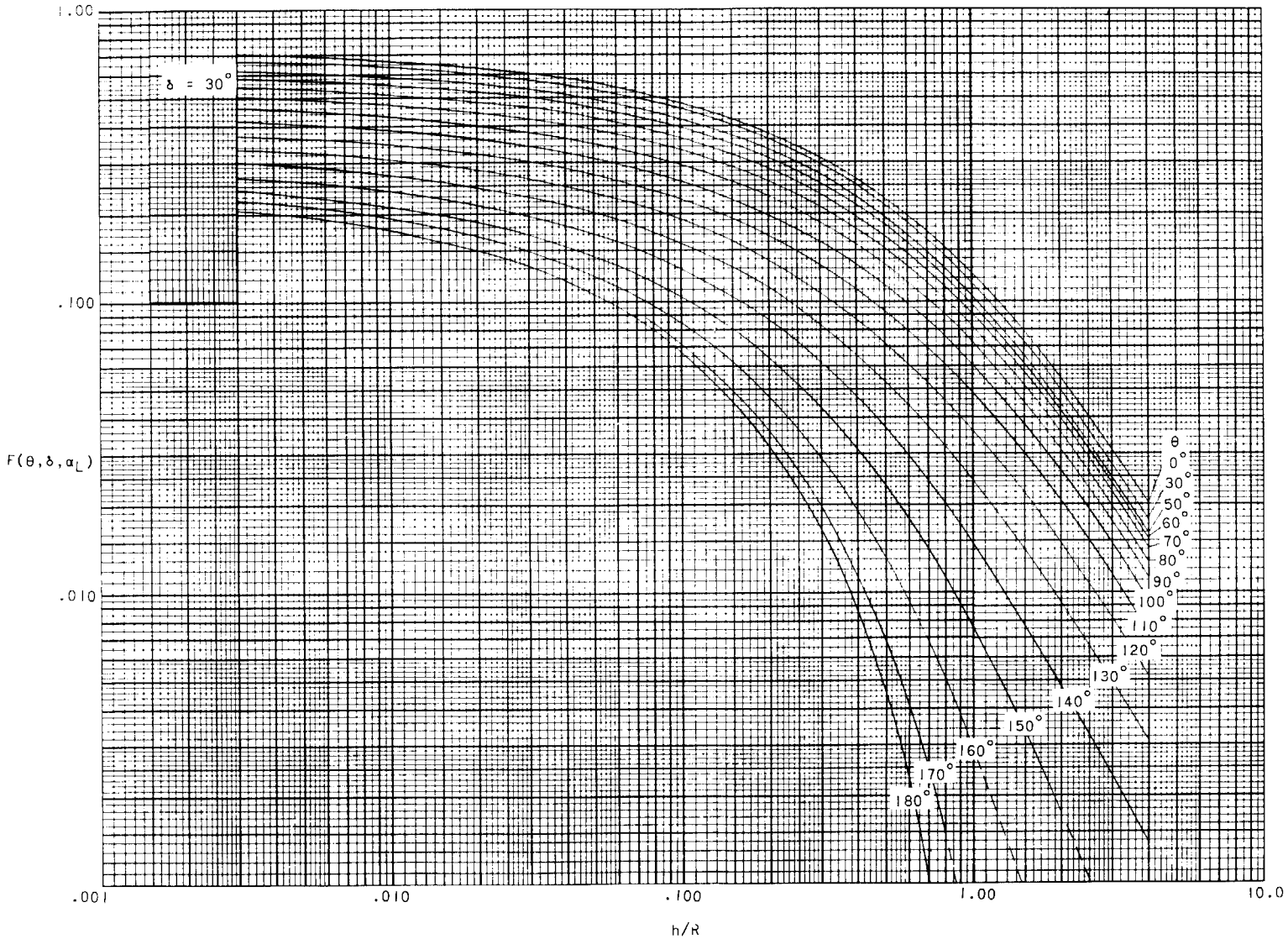

(c) $\delta = 30^{\circ}$.

Figure 5.- Continued.

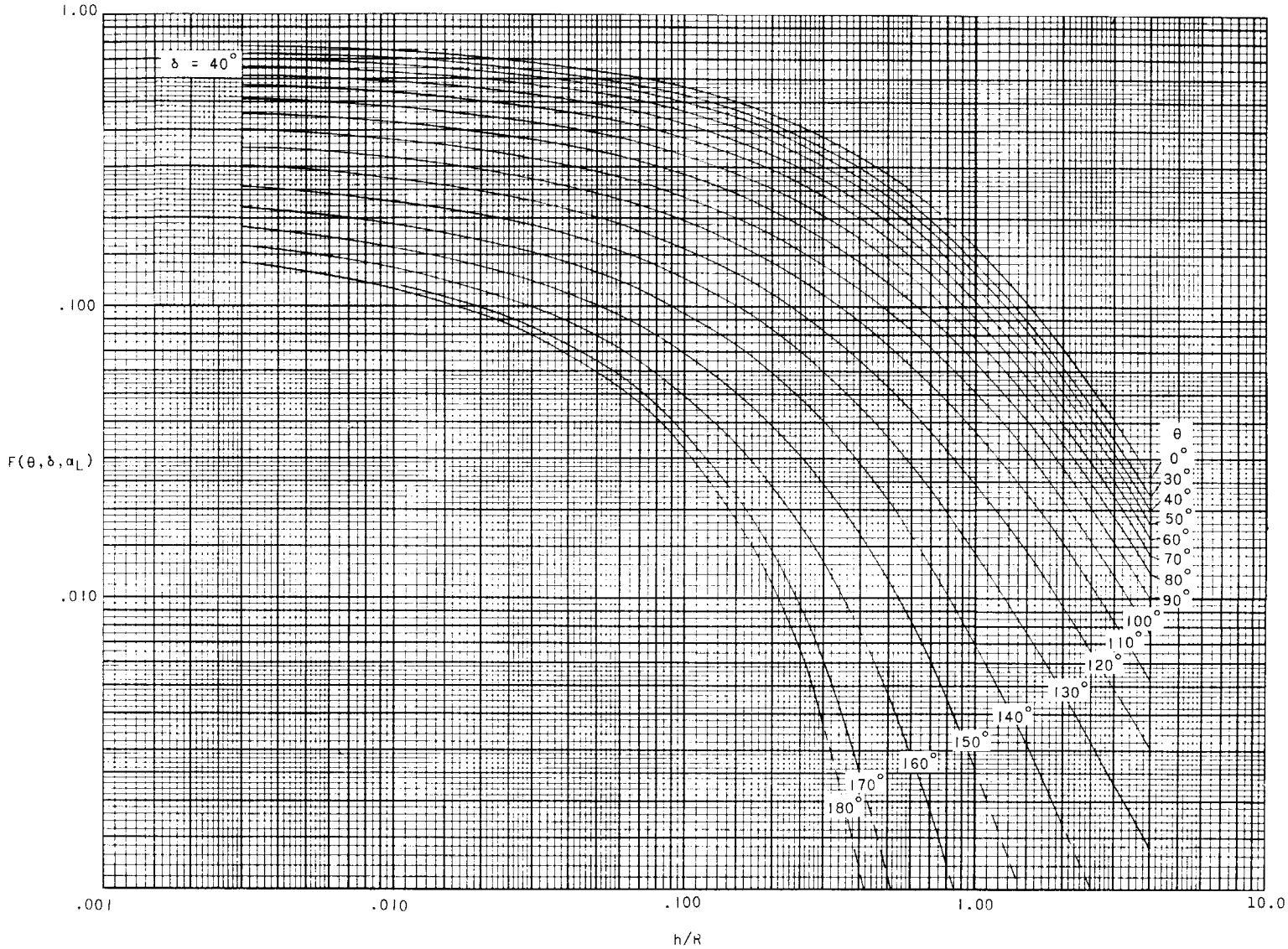

(d) $\delta = 40°$.

Figure 5.- Continued.

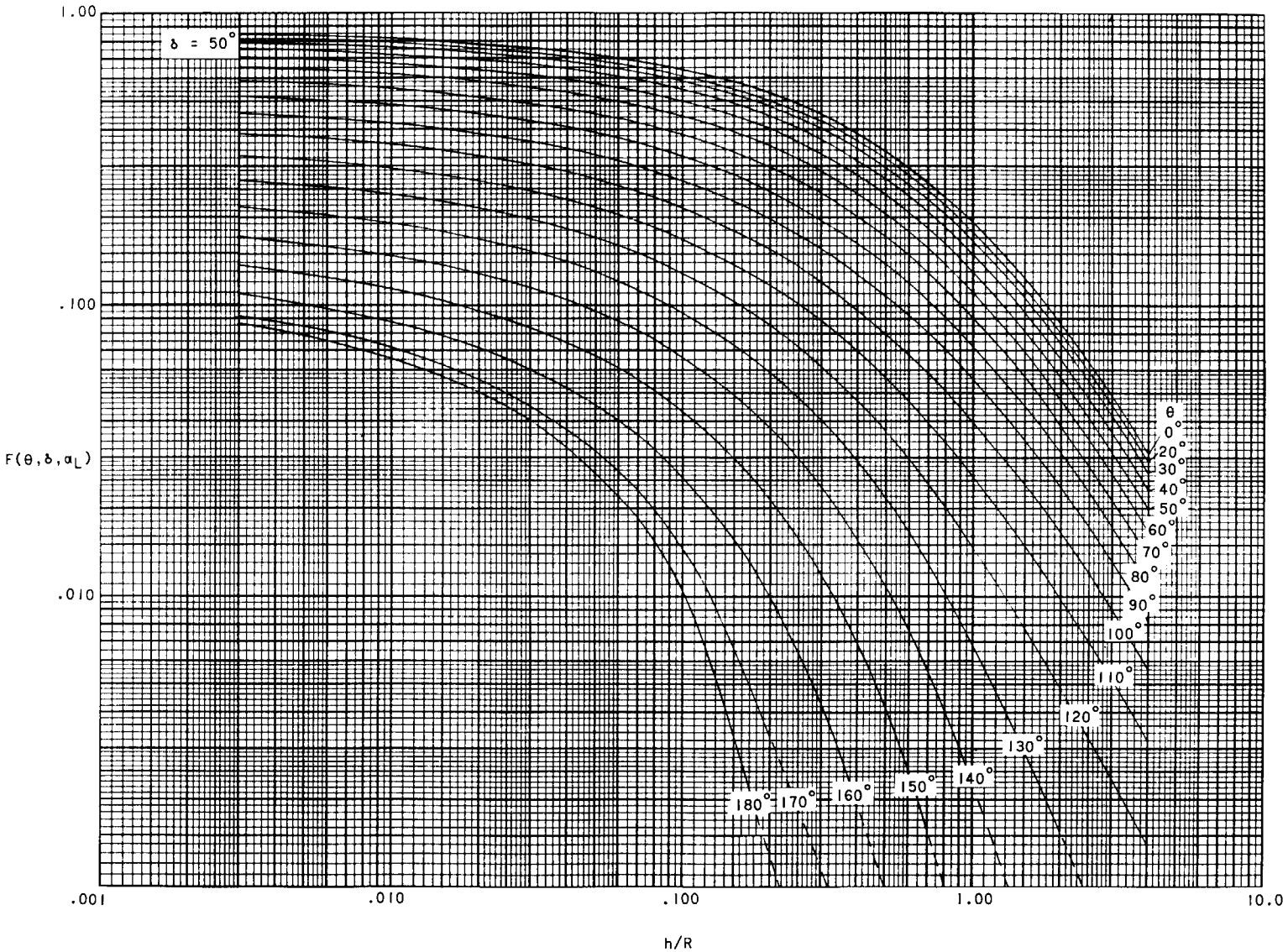

(e) $\delta = 50^{\circ}$.

Figure 5.- Continued.

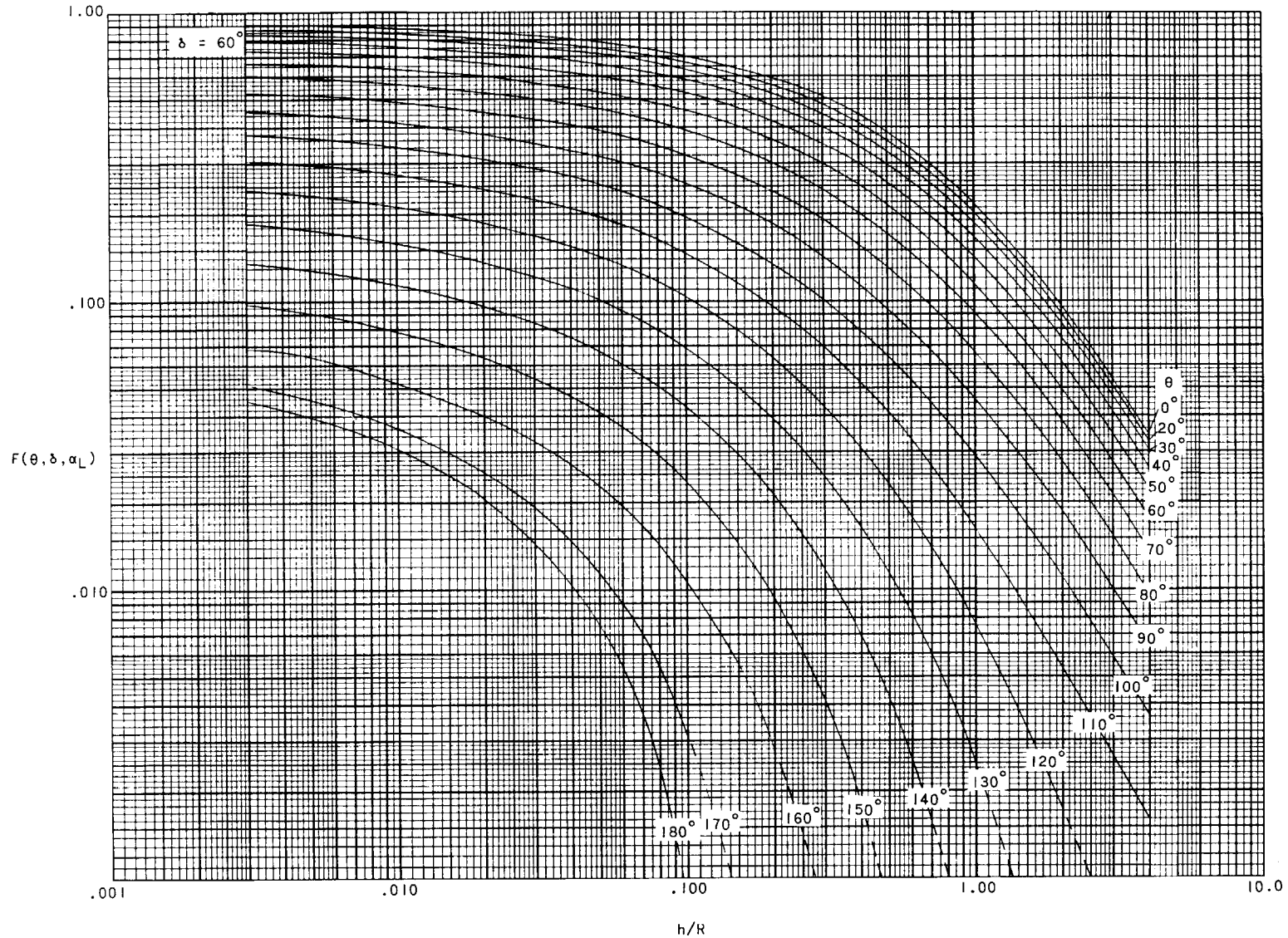

(f) $\delta = 60^{o}$.

Figure 5.- Continued.

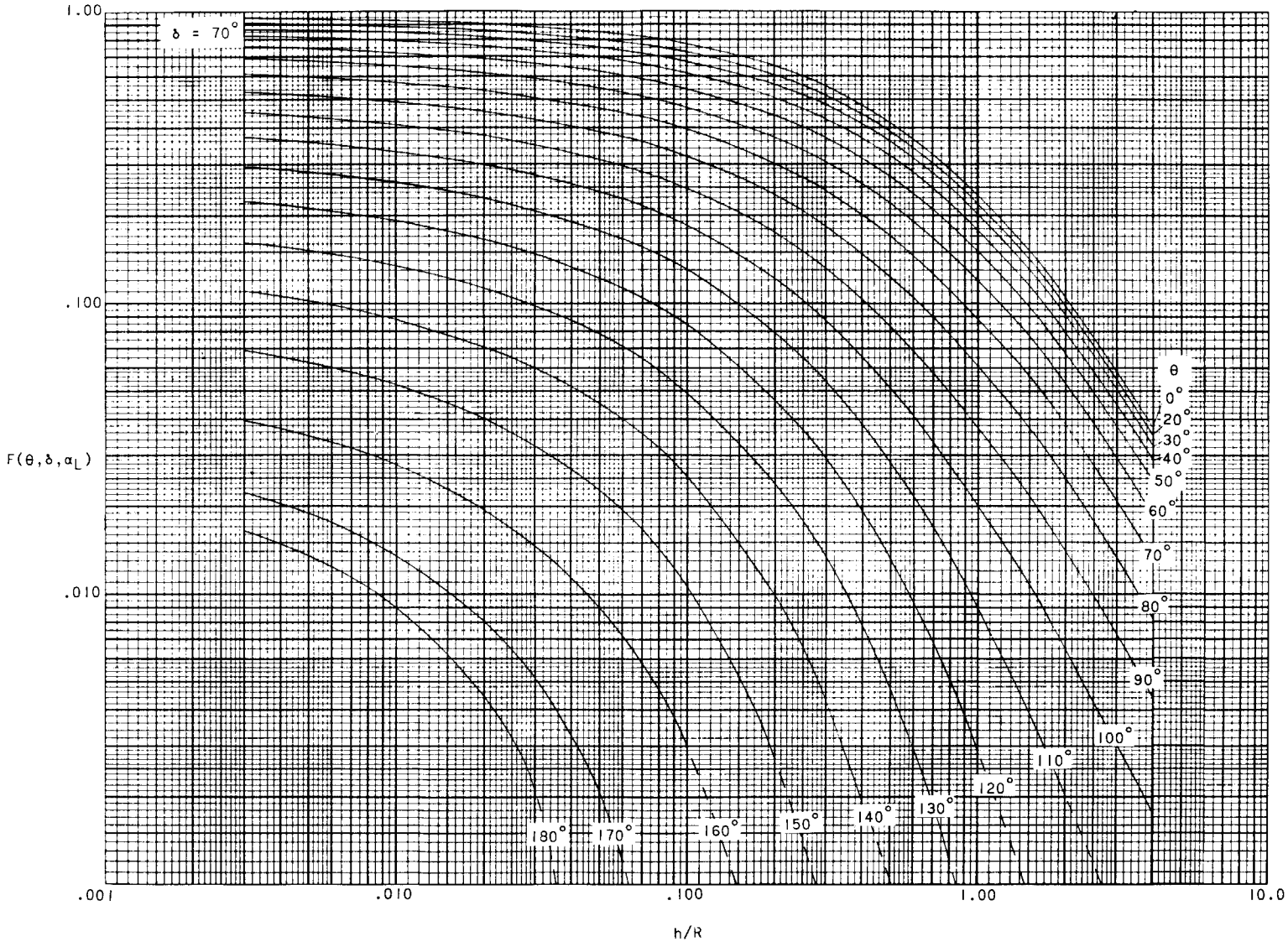

(g) $\delta = 70^{\circ}$.

Figure 5.- Continued.

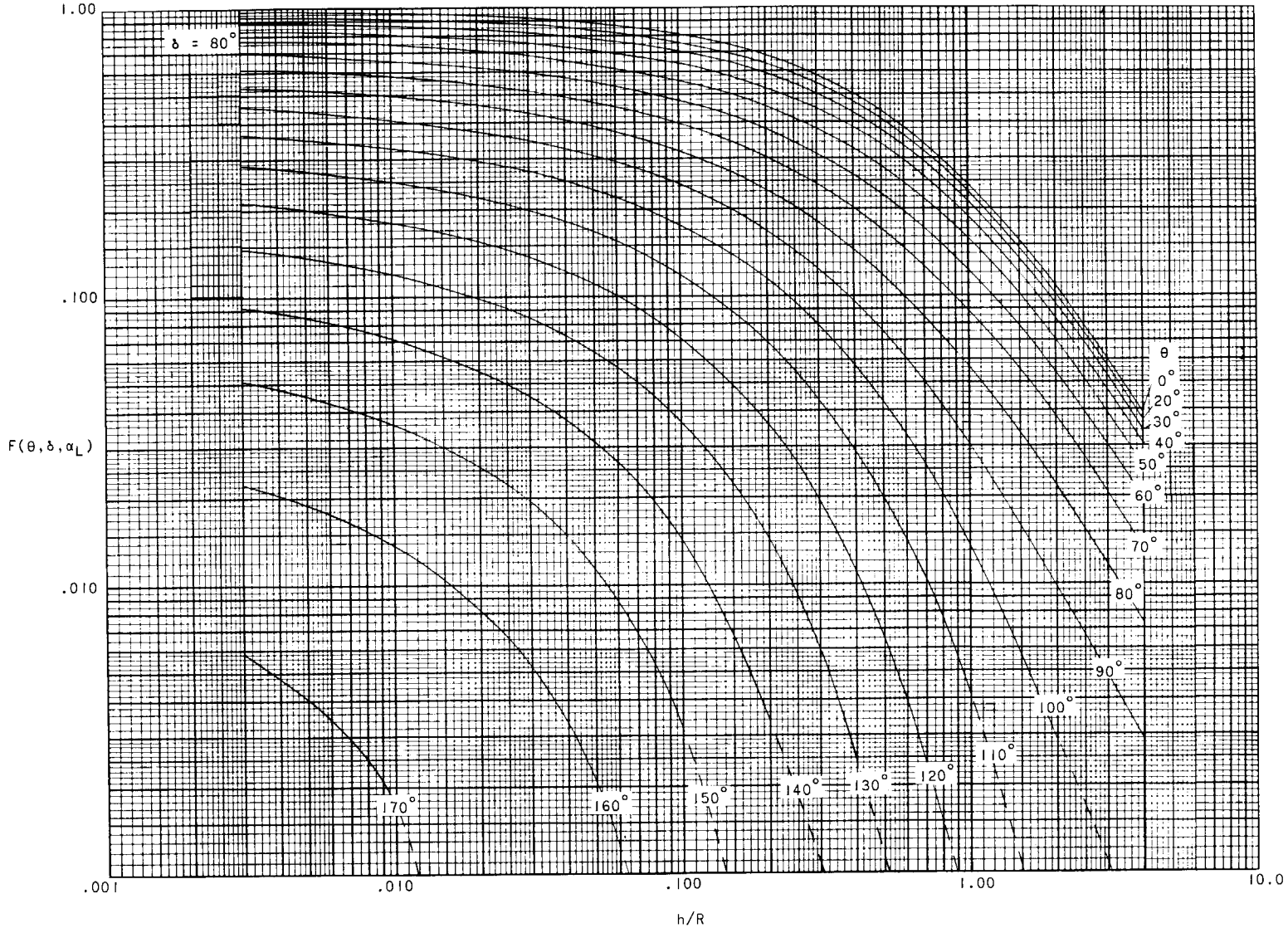

(h) $\delta = 80°$.

Figure 5.- Concluded.

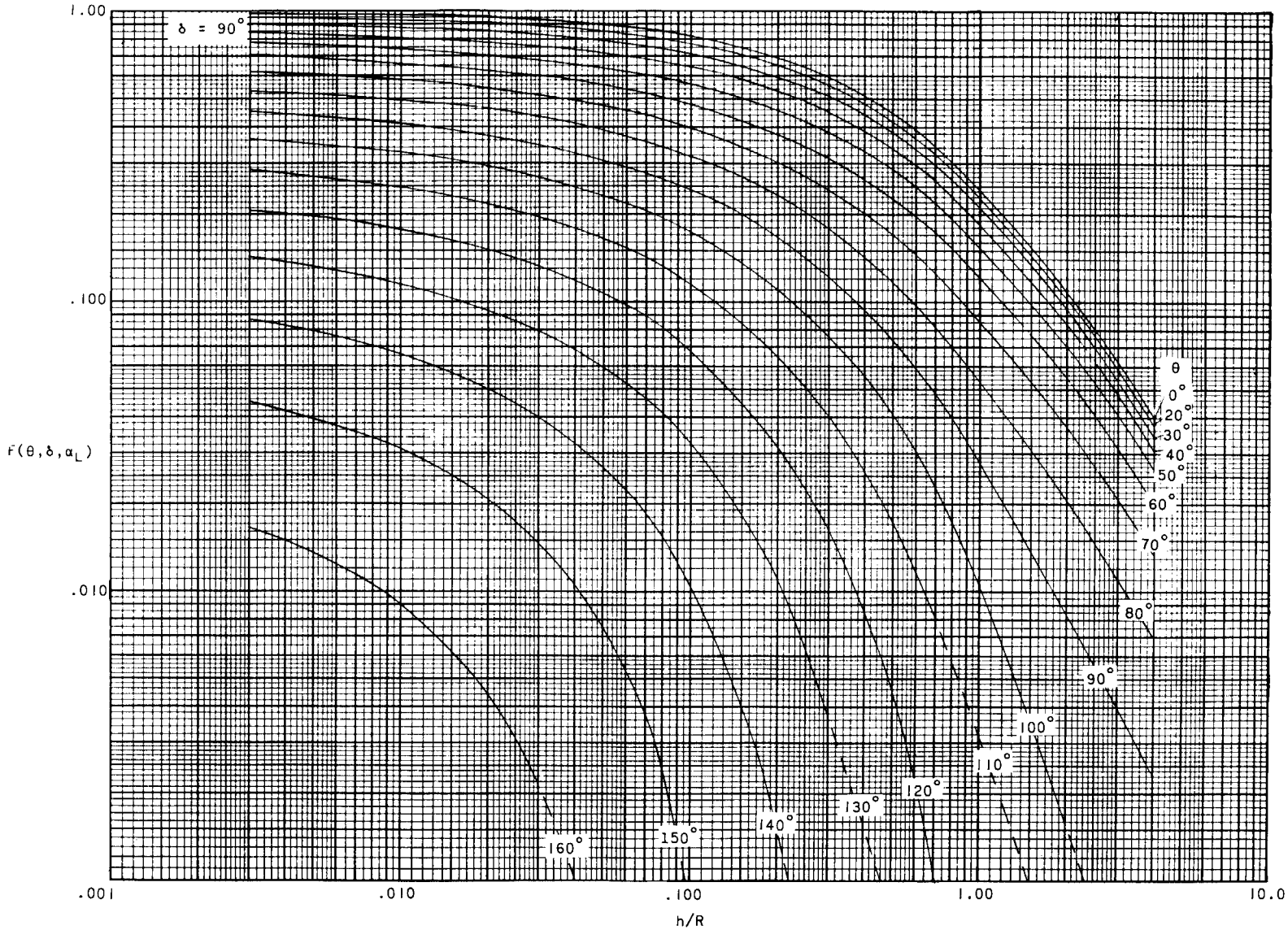

Figure 6.- Instantaneous geometric shape factor for a flat plate ($\delta = 90^{\circ}$) as a function of altitude and attitude.

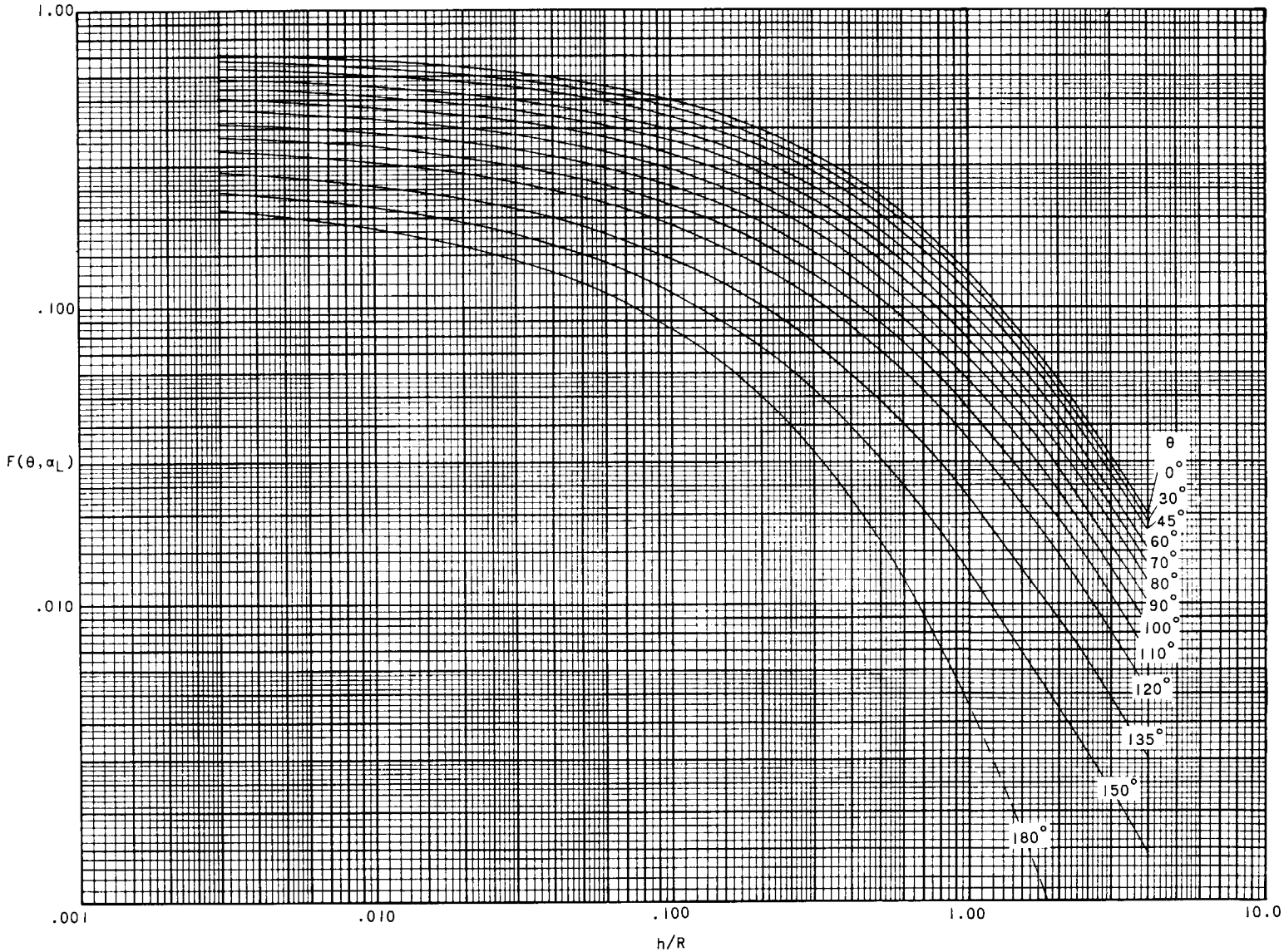

Figure 7.- Instantaneous geometric shape factor for a hemisphere as a function of altitude and attitude.

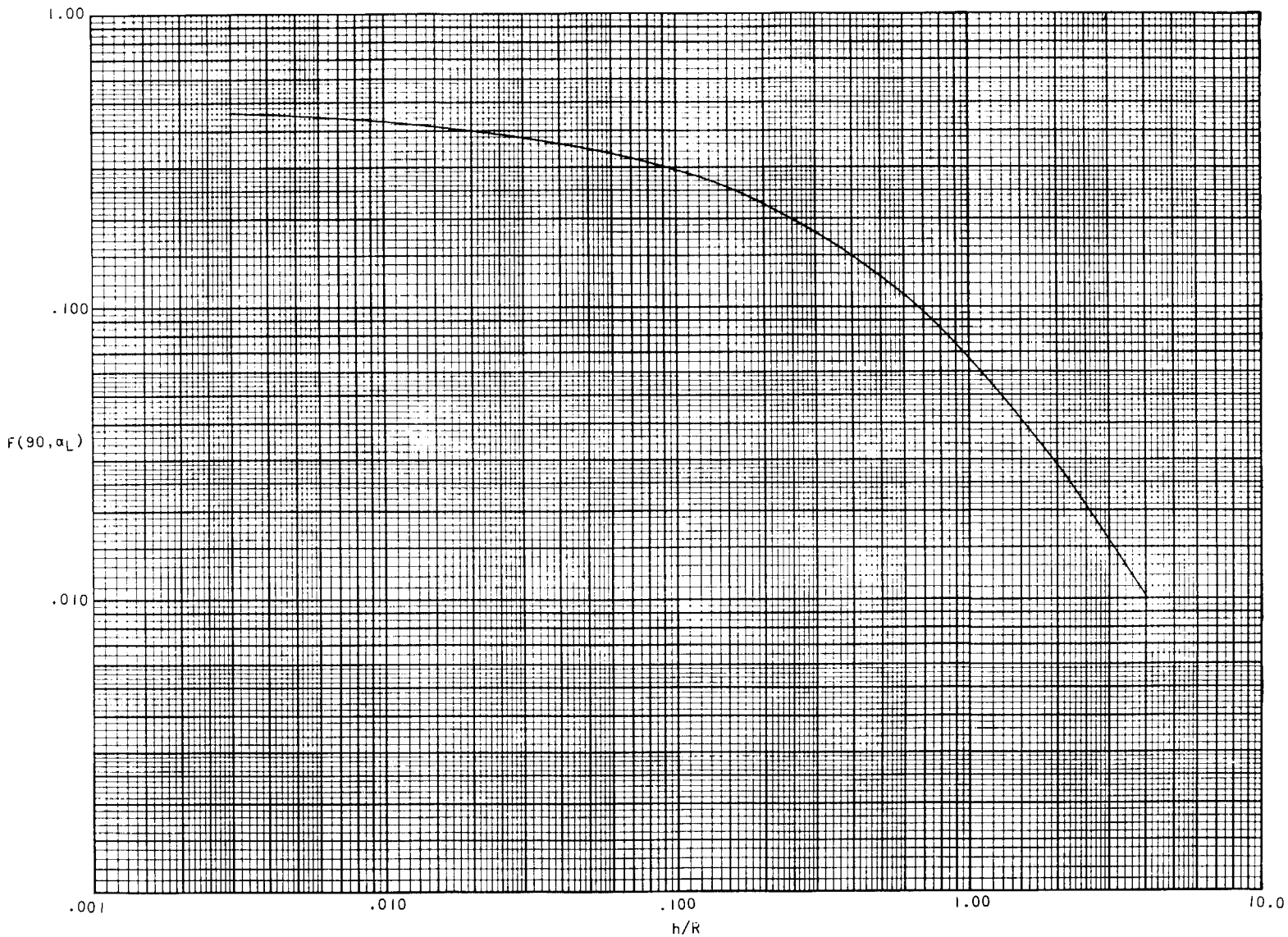

Figure 8.- Geometric shape factor for a sphere as a function of altitude.

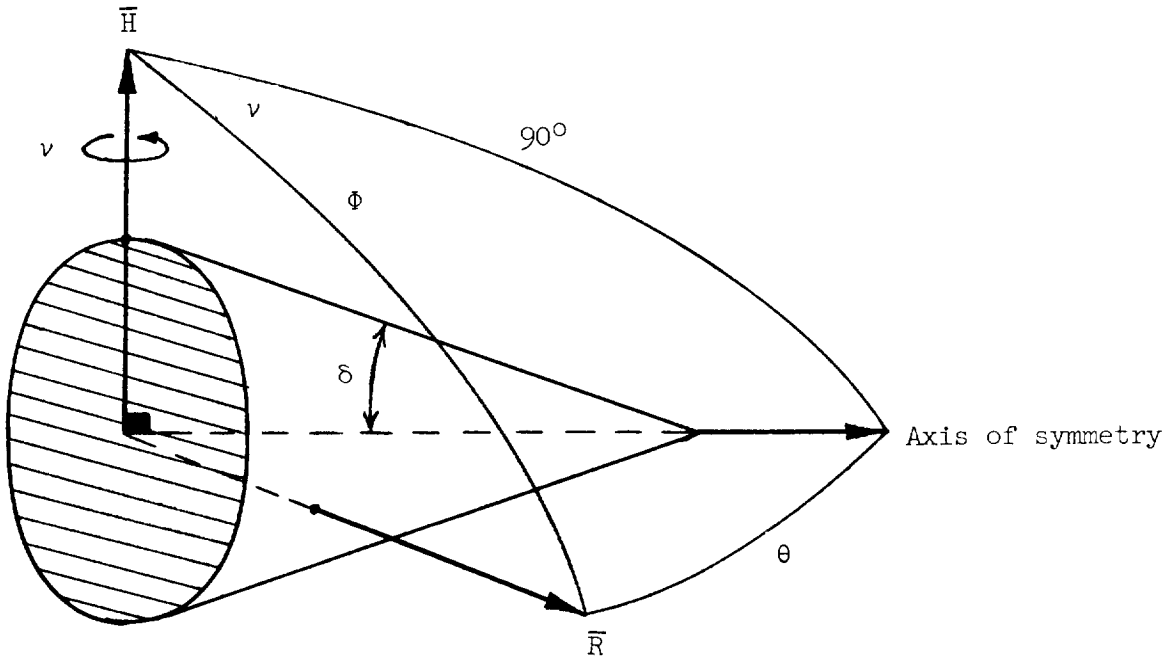

Figure 9.- Orientation geometry for a body of revolution.

Figure 10.- Geometric shape factor for a spinning right circular cylinder ($\delta = 0^{\circ}$) as a function of altitude and attitude.

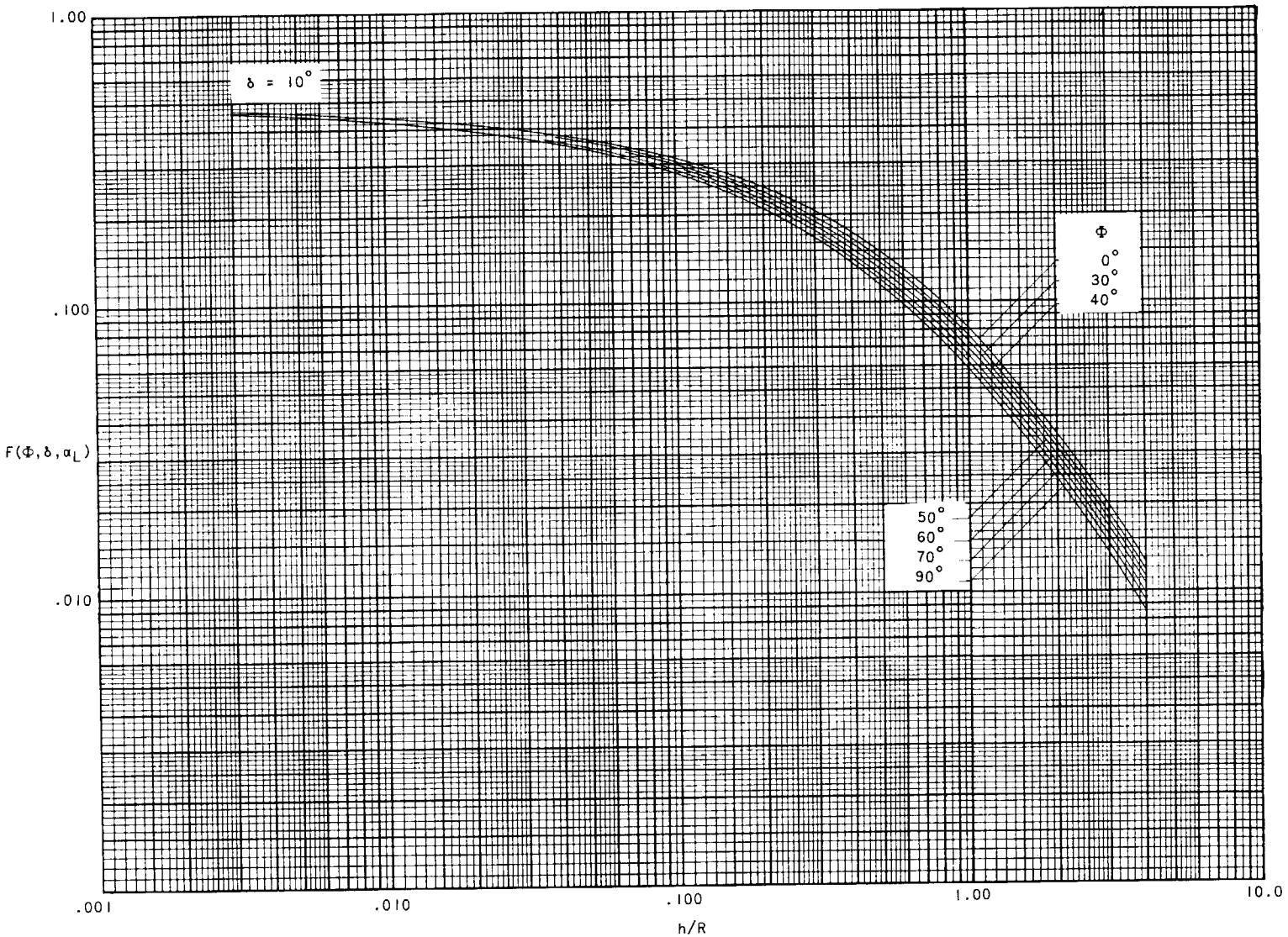

(a) $\delta = 10^{\circ}$.

Figure 11.- Geometric shape factor for a spinning cone as a function of altitude and attitude.

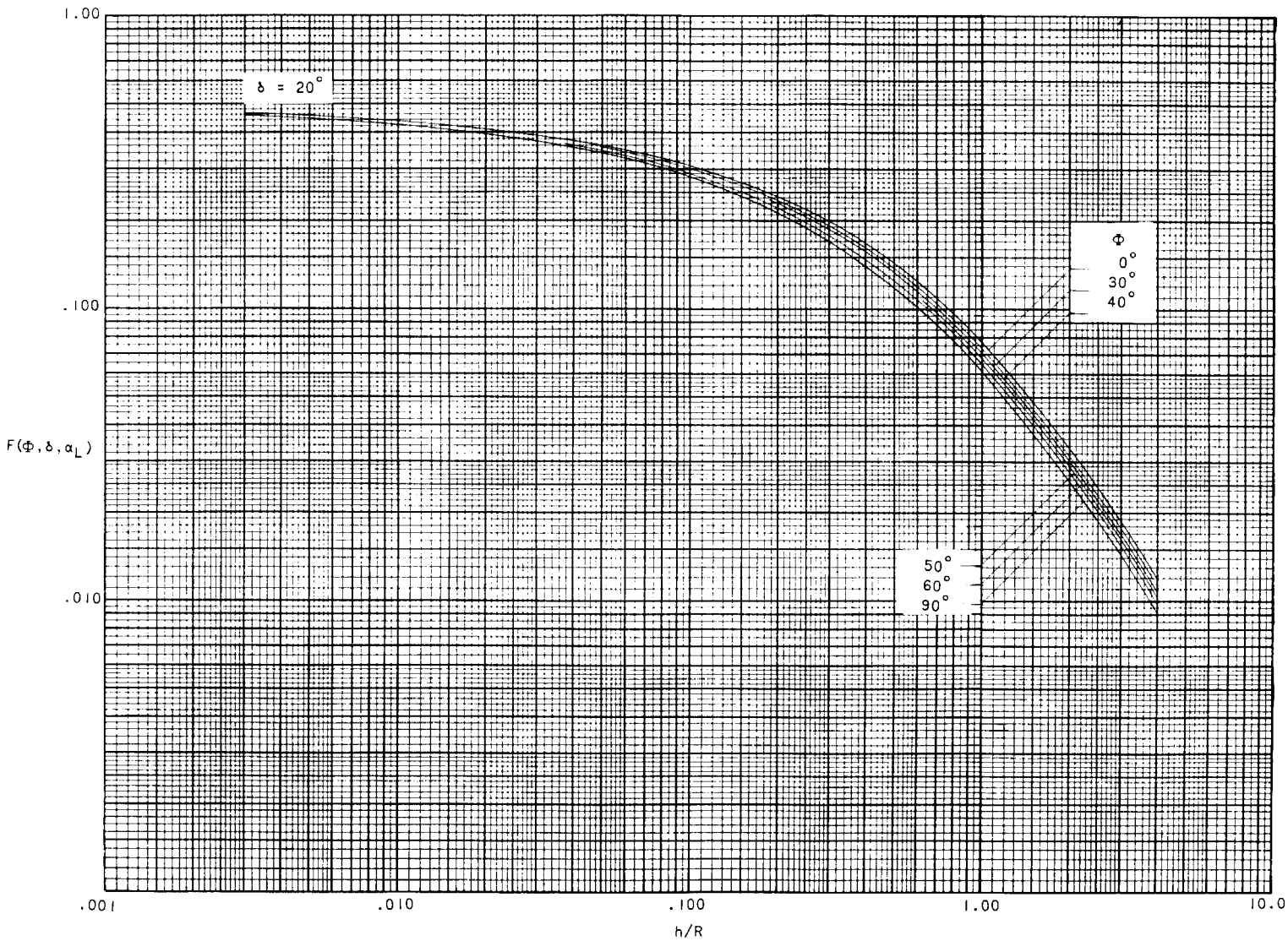

(b) $\delta = 20^{\circ}$.

Figure 11.- Continued.

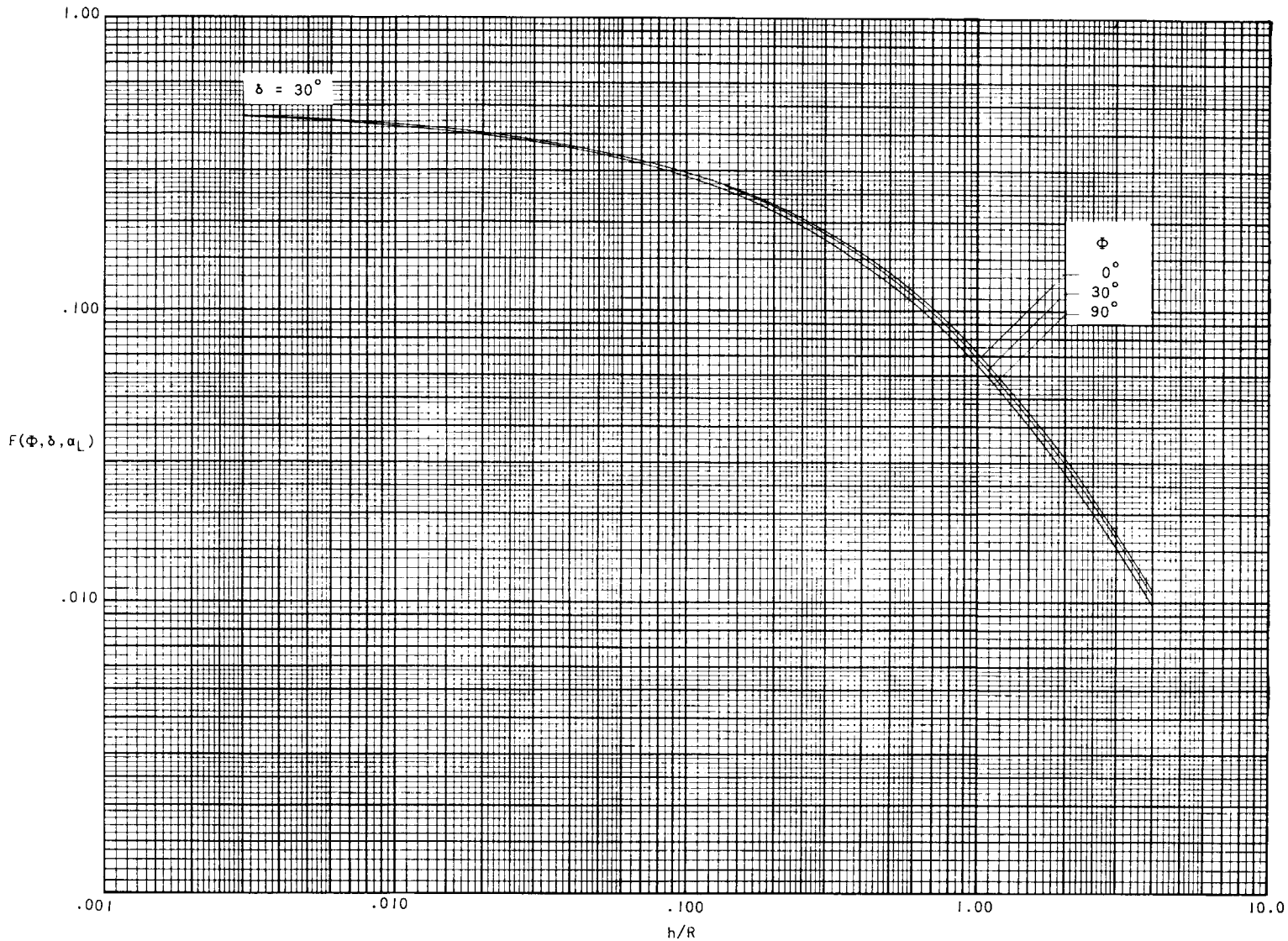

(c) $\delta = 30^{\circ}$.

Figure 11.- Continued.

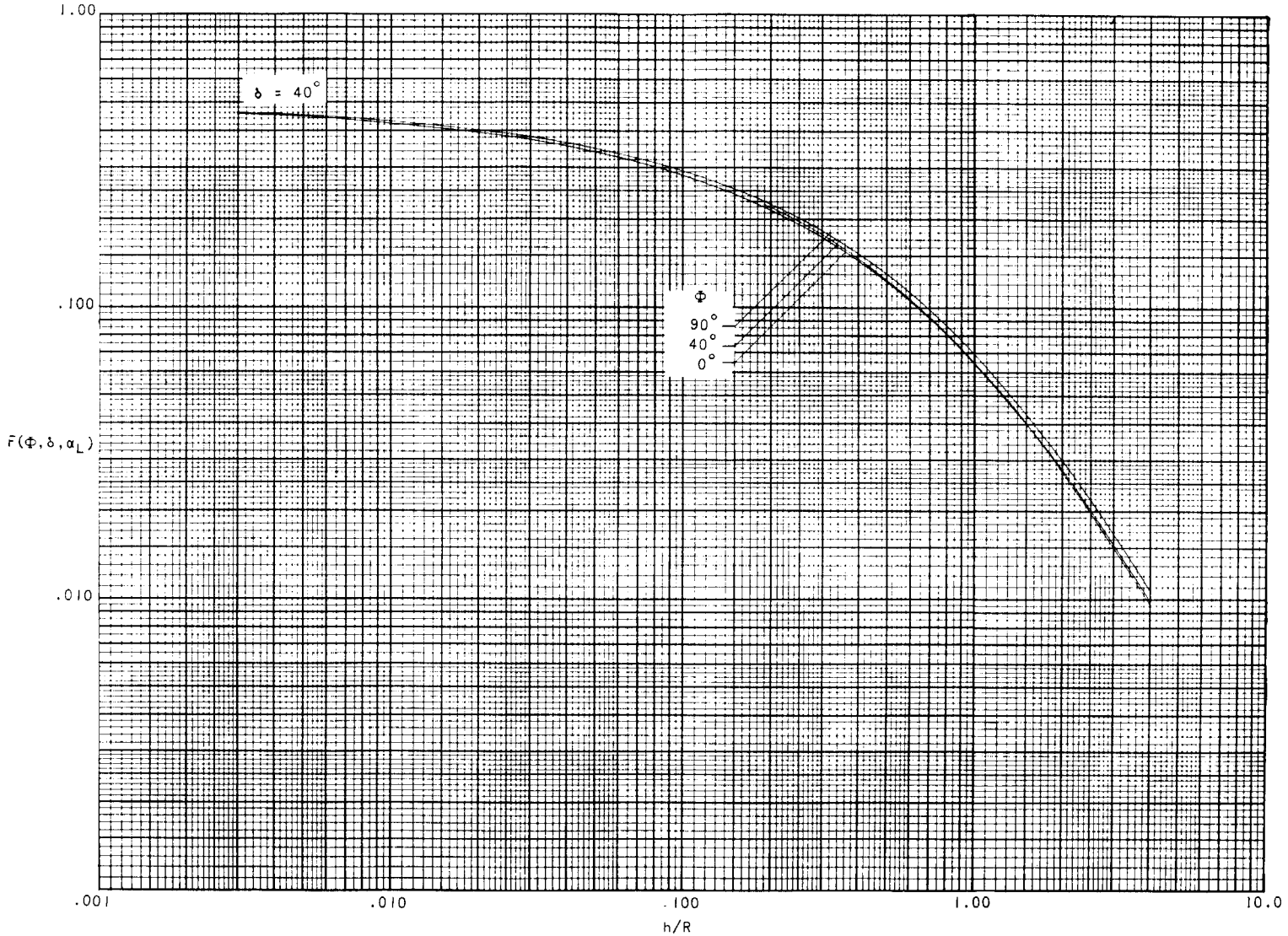

(d) $\delta = 40^{\circ}$.

Figure 11.- Continued.

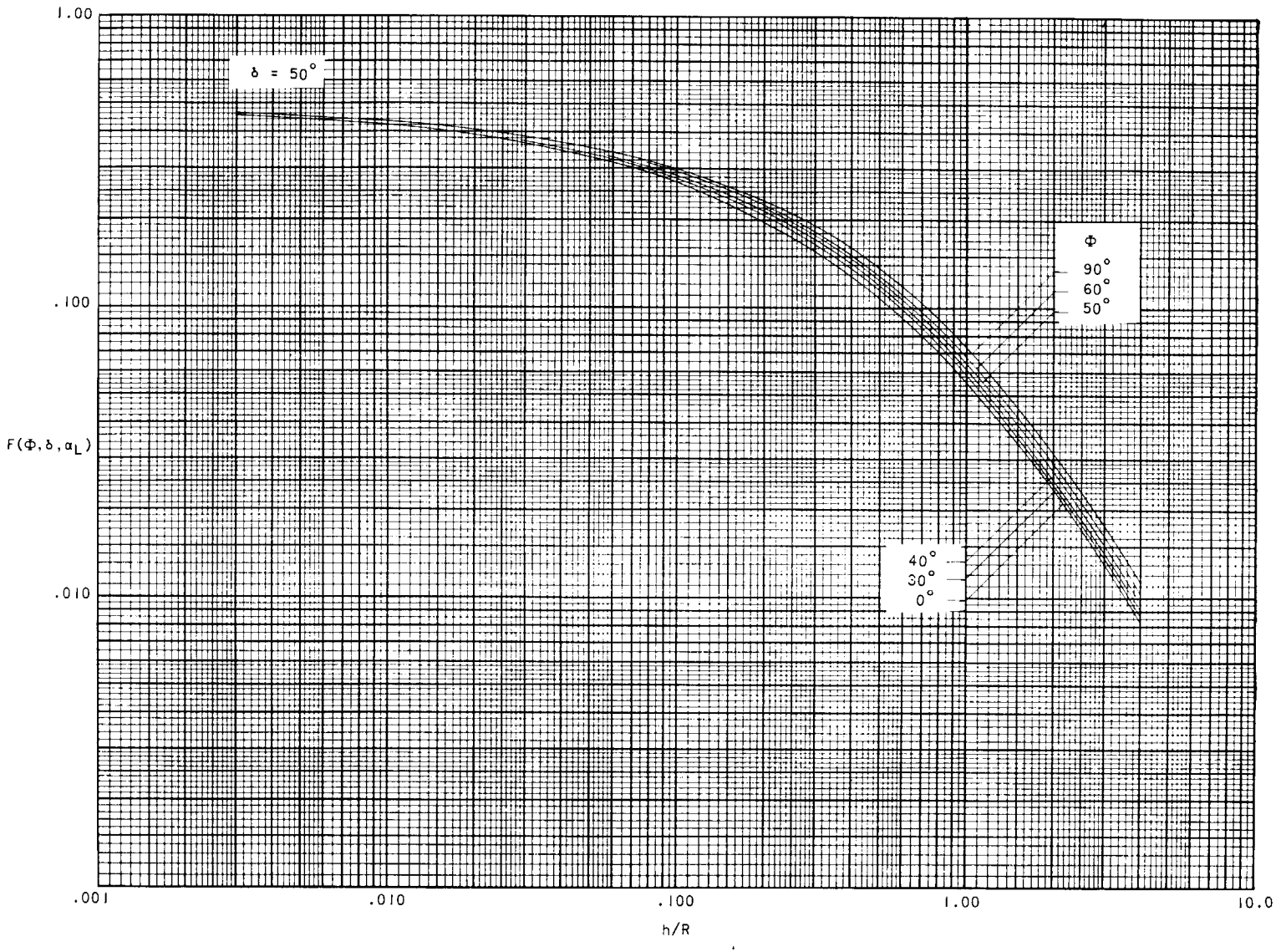

(e) $\delta = 50^{\circ}$.

Figure 11.- Continued.

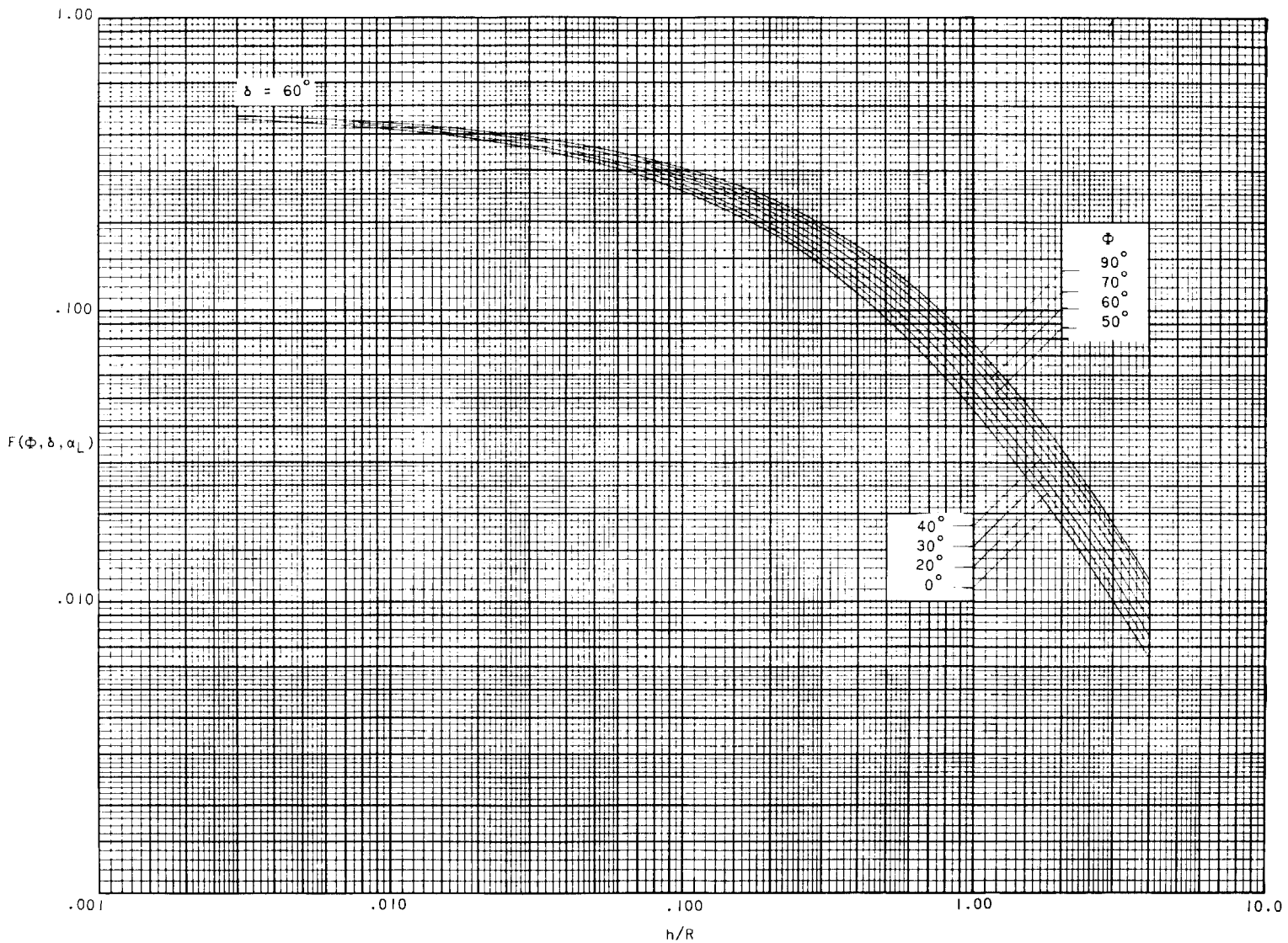

(f) $\delta = 60^\circ$.

Figure 11.- Continued.

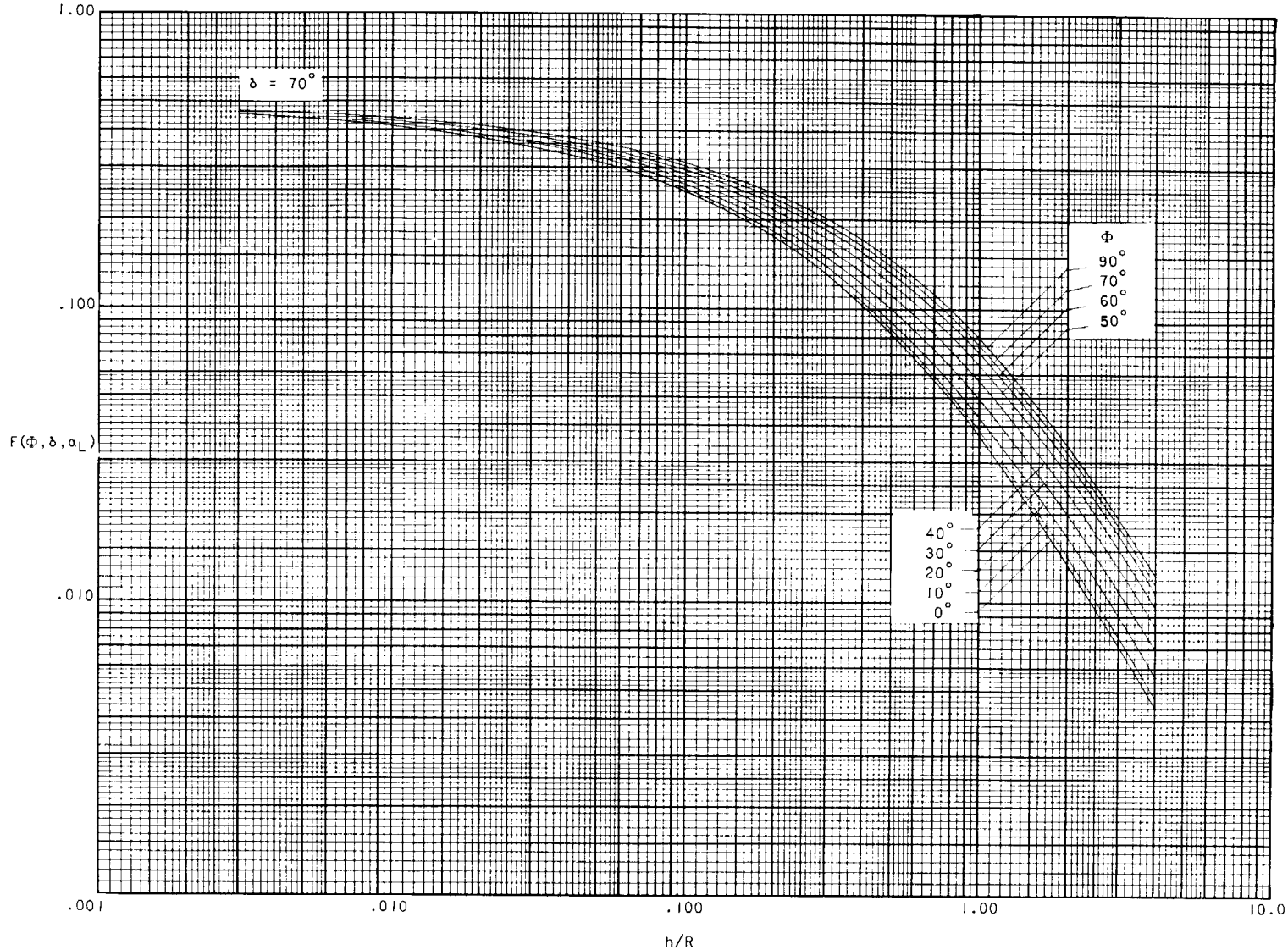

(g) $\delta = 70^{\circ}$.

Figure 11.- Continued.

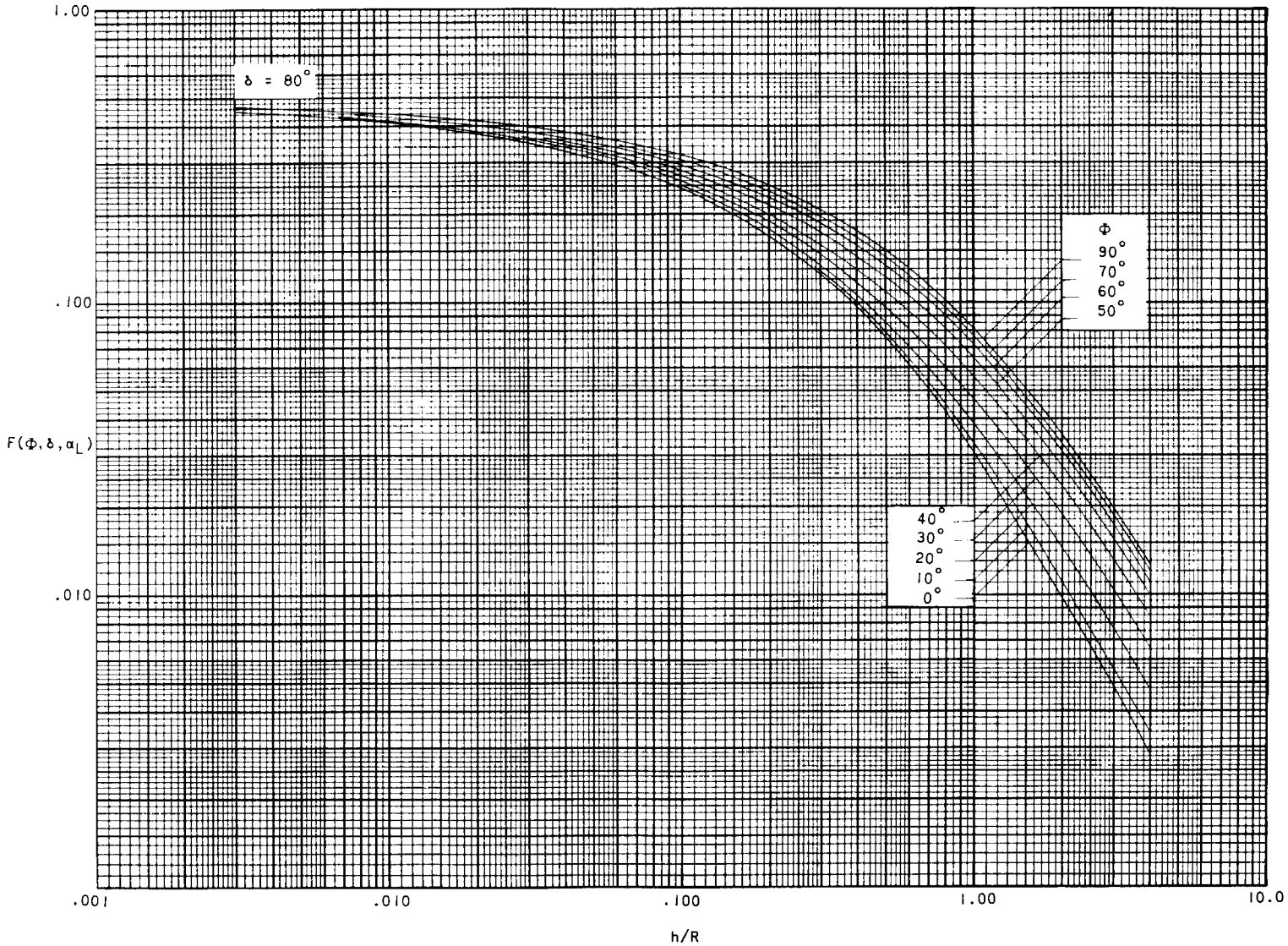

(h) $\delta = 80^{\circ}$.

Figure 11.- Concluded.

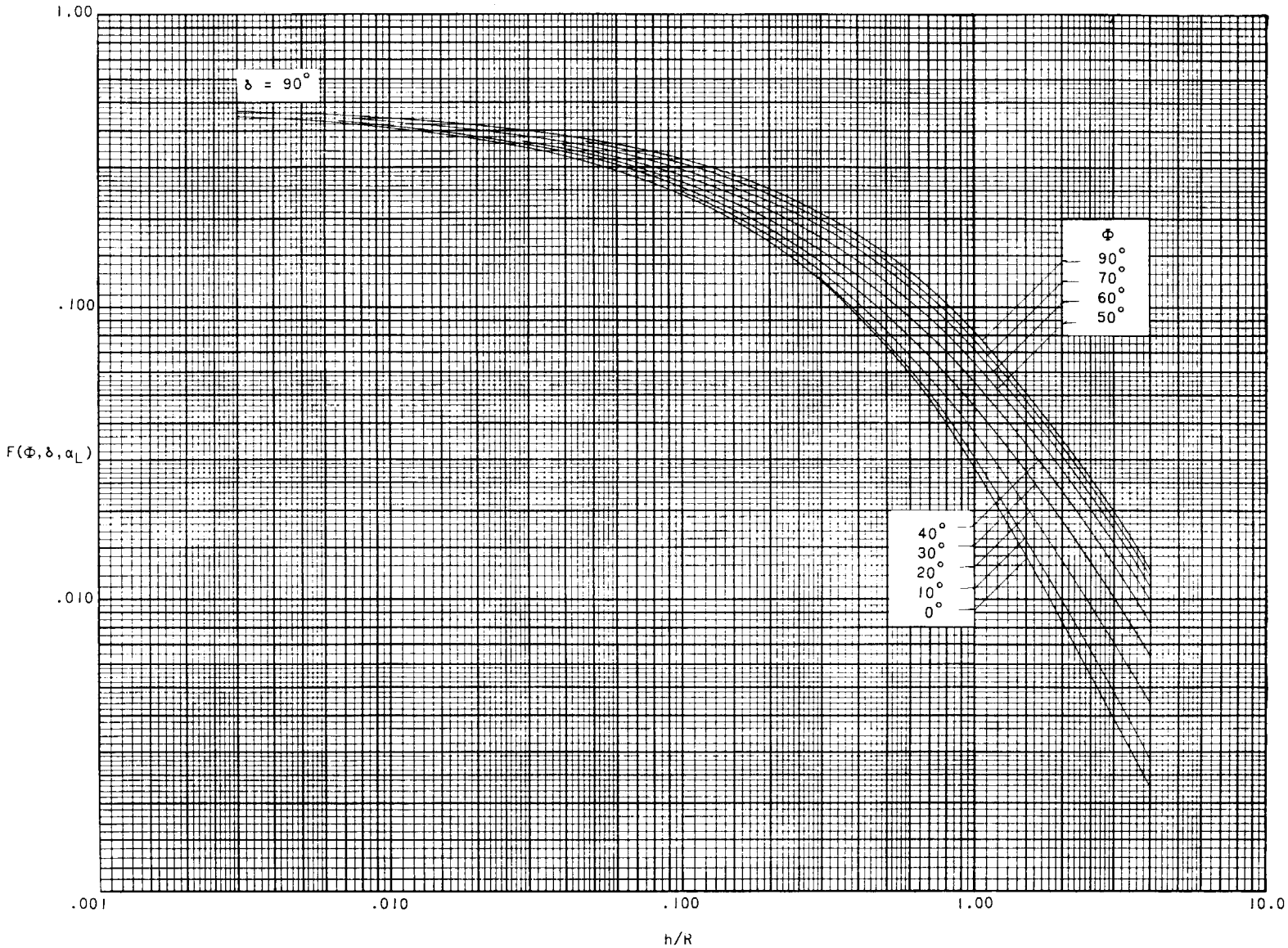

Figure 12.- Geometric shape factor for a spinning flat plate ($\delta = 90^{\circ}$) as a function of altitude and attitude.

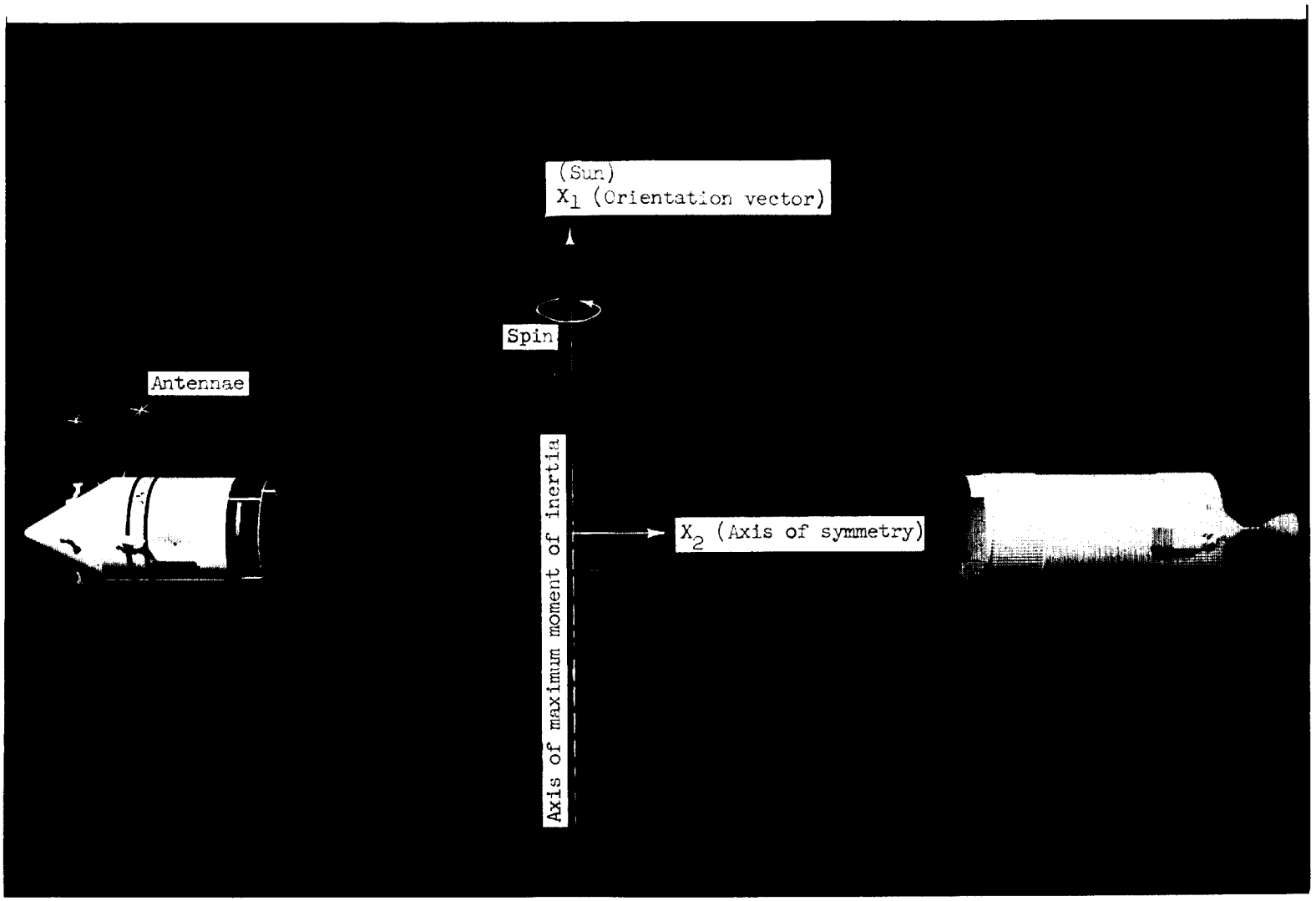

Figure 13.- Spinning configuration of a manned orbital research laboratory. L-64-3723.1

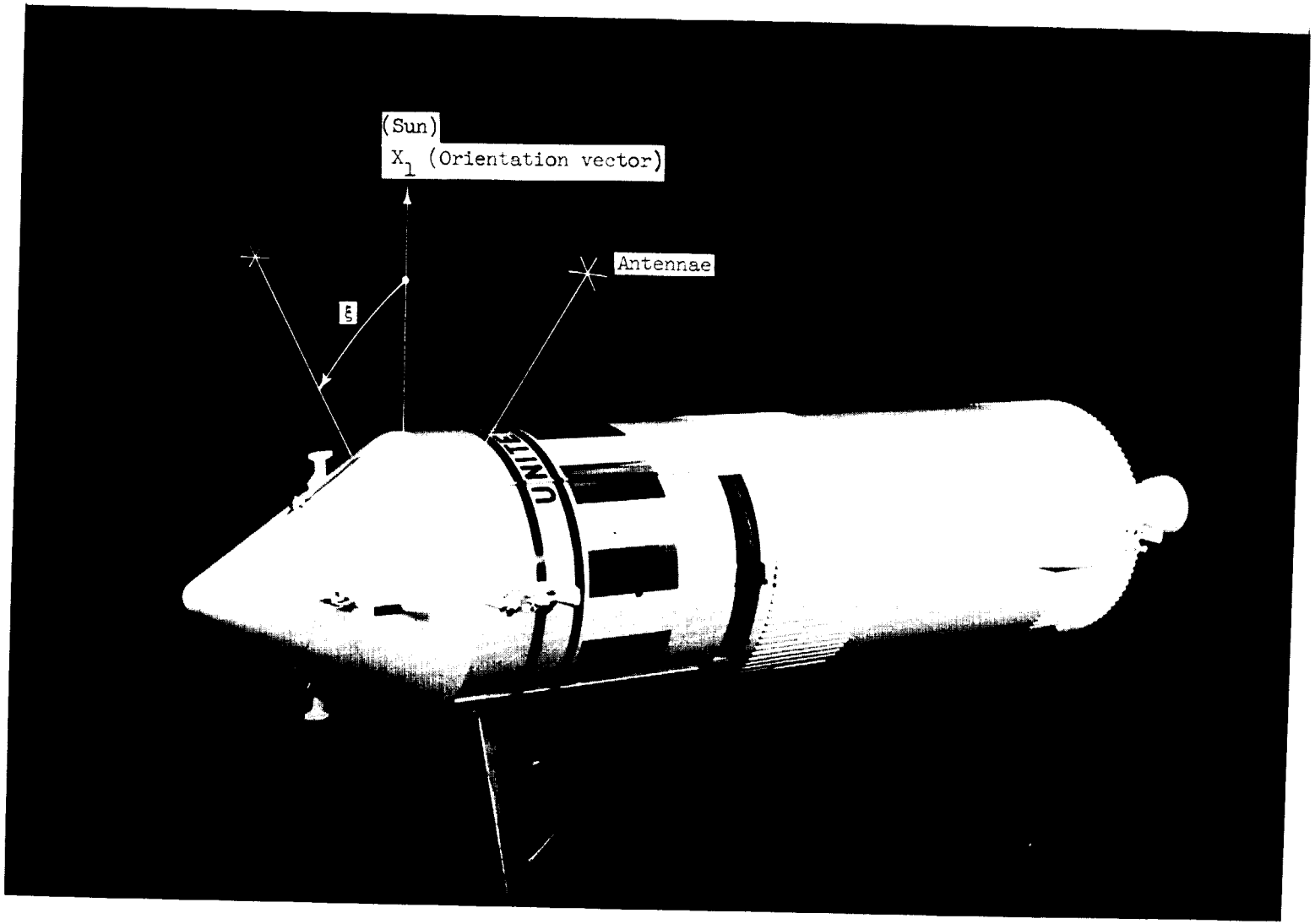

Figure 14.- Nonspinning configuration of a manned orbital research laboratory. L-64-3722.1

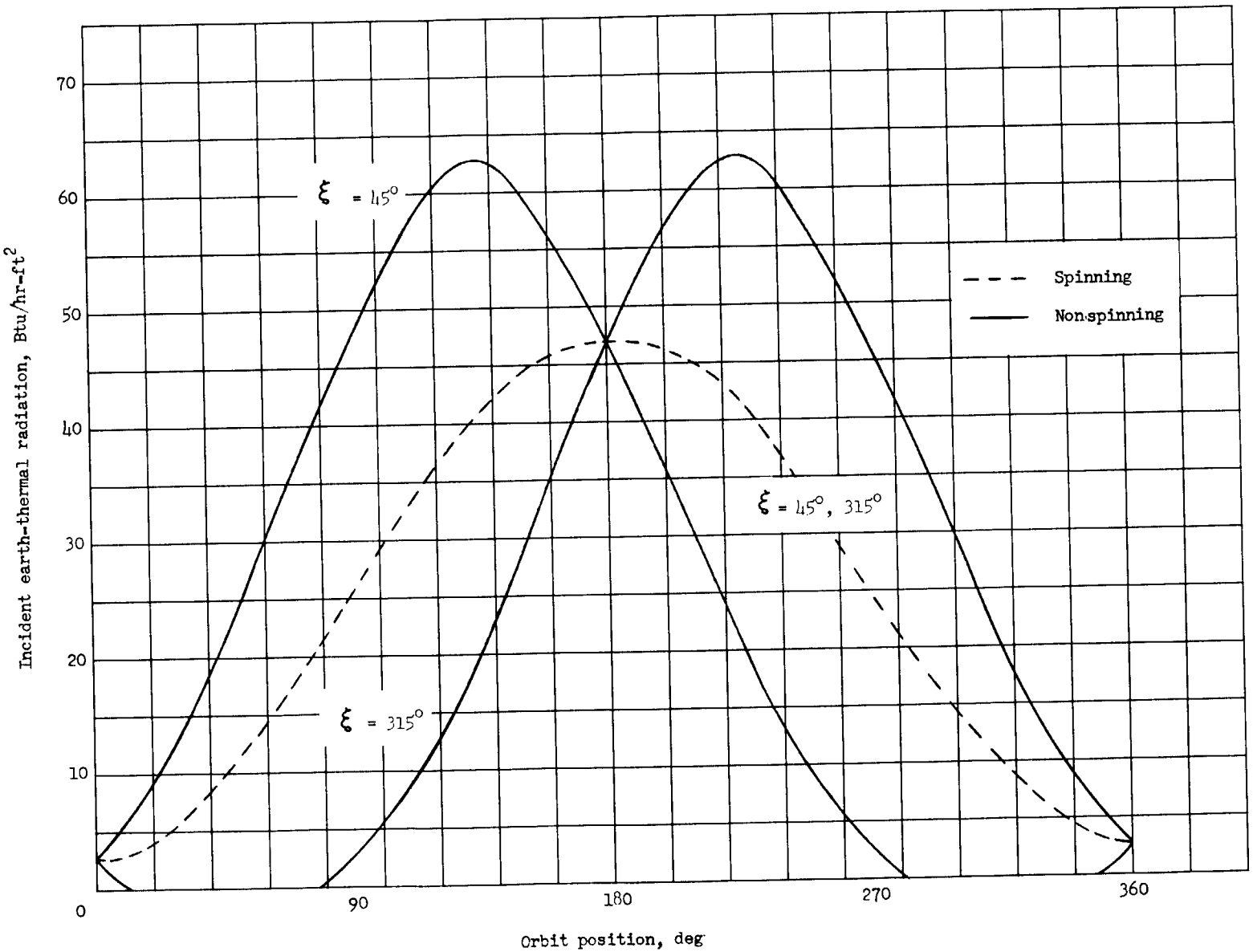

Figure 15.- Incident earth-thermal radiation to antennae locations as a function of orbit position for spinning and nonspinning modes of vehicle operation.

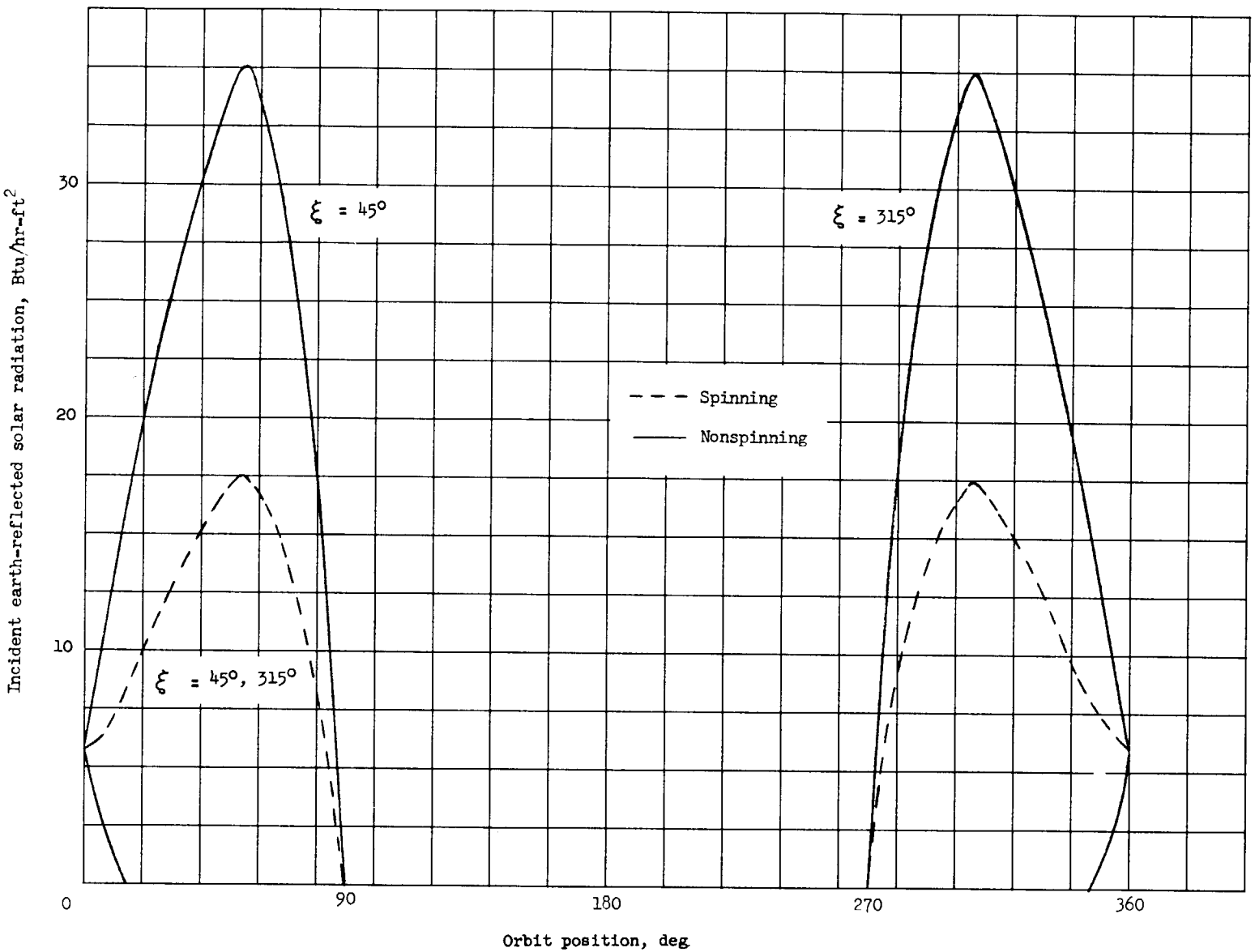

Figure 16.- Incident earth-reflected solar radiation to antennae locations as a function of orbit position for spinning and nonspinning modes of vehicle operation.